

Supporting Information

Ligand electronic fine-tuning and its repercussion on the photocatalytic activity and mechanistic pathways of the copper-photocatalysed aza-Henry Reaction

Chenfei Li,^a Robert Dickson,^a Nils Rockstroh,^b Jabor Rabeah,^b David B. Cordes,^a Alexandra M. Z. Slawin,^a Paul Hünemörder,^b Anke Spannenberg,^b Michael Bühl,^a Esteban Mejía,^{b*} Eli Zysman-Colman,^{a*} and Paul C. J. Kamer.^{b*}

^aOrganic Semiconductor Centre, EaStCHEM School of Chemistry, University of St Andrews, North Haugh, KY16 9ST St Andrews, United Kingdom

^bLeibniz Institute for Catalysis, Albert-Einstein-Str. 29a, 18059 Rostock, Germany

esteban.mejia@catalysis.de
eli.zysman-colman@st-andrews.ac.uk
paul.kamer@catalysis.de

Contents

1.	General information	3
	General procedure	3
	[Cu(neocuproine)(<i>p</i> -CF ₃ -xantphos)]PF ₆ ([1]PF ₆)	3
	[Cu(neocuproine)(<i>p</i> -F-xantphos)]PF ₆ ([2]PF ₆)	4
	[Cu(neocuproine)(xantphos)]PF ₆ ([3]PF ₆)	4
	[Cu(neocuproine)(<i>p</i> -Me-xantphos)]PF ₆ ([4]PF ₆)	5
	[Cu(neocuproine)(<i>p</i> -OMe xantphos)]PF ₆ ([5]PF ₆)	5
2.	<i>In-situ</i> synthesis of photocatalyst [3]PF ₆	5
3.	X-Ray Diffraction.....	7
4.	EPR Measurements	8
5.	Photophysics.....	8
6.	Electrochemistry.....	11
7.	Computational Details.....	12
	Results with other functionals.....	14
8.	Photocatalysis.....	15
	General procedure	15
	Screening of reaction conditions.....	16
9.	Mechanistic studies:	16

10.	Comparison between BF ₄ ⁻ and PF ₆ ⁻	20
11.	NMR of the Synthesized of complexes	22
	[Cu(dmphen)(p-CF ₃ -xantphos)]PF ₆ ([1]PF ₆)	22
	[Cu(dmphen)(p-F xantphos)] PF ₆ ([2]PF ₆)	24
	[Cu(dmphen)(p-H xantphos)] PF ₆ ([3]PF ₆)	25
	[Cu(dmphen)(p-Me xantphos)] PF ₆ ([4]PF ₆).....	28
	[Cu(dmphen)(p-OMe xantphos)] PF ₆ ([5]PF ₆).....	30
12.	Optimized coordinates of complexes 1 - 5 (PBE0-D3/ECP1 optimized), xyz format	32
	Complex 1.....	32
	Complex 2.....	34
	Complex 3.....	35
	Complex 4.....	37
	Complex 5.....	39
	References.....	42

1. General information

All reactions were carried out using standard Schlenk techniques under argon atmosphere. All glassware was dried at 130 °C overnight and cooled under vacuum prior to use. ^1H , $^{13}\text{C}-\{\text{H}\}$ and $^{31}\text{P}-\{\text{H}\}$ Nuclear Magnetic Resonance (NMR) spectra were recorded at 298K on either Bruker Avance 300, Avance II 400 and Bruker Avance II 500 spectrometers using the residual solvent peak for ^1H and $^{13}\text{C}-\{\text{H}\}$ as reference. All NMR shifts are reported as δ in parts per million (ppm). A Gallenkamp melting point apparatus was used to determinate melting points. Toluene was distilled from sodium, THF and diethyl ether were distilled from sodium/benzophenone, hexanes from sodium/benzophenone/triglyme and dichloromethane and acetonitrile from calcium hydride. Aqueous reagents were degassed under argon before use for a minimum period of four hours. All reagents were purchased from commercial suppliers and used as received, unless otherwise noted. The xantphos ligands ($\text{P}^\wedge\text{P} = 4,5\text{-Bis}(di-p\text{-trifluoromethylphenylphosphino)-9,9-dimethylxanthene}$: $p\text{-CF}_3\text{-xantphos}$; $4,5\text{-bis}(di-p\text{-fluorophenylphosphino)-9,9-dimethylxanthene}$: $p\text{-F-xantphos}$; $4,5\text{-bis}(di-p\text{-tolylphosphino)-9,9-dimethylxanthene}$: $p\text{-Me-xantphos}$; $4,5\text{-bis}(di-p\text{-anisylphosphino)-9,9-dimethylxanthene}$: $p\text{-OMe-xantphos}$; were synthesized by modified literature procedures.¹⁻³ Mass spectrometry was carried out at the Leibniz Institute for Catalysis – LIKAT.

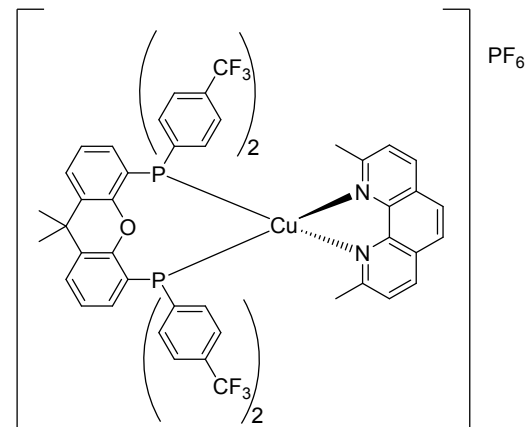
Synthesis and characterization of compounds

General procedure

A three-necked, round-bottomed 250 mL SCHLENK flask equipped with a magnetic stirring bar is heated up with a heat gun under vacuum and flushed with Argon. The procedure is repeated for three times. The whole reaction is carried out under inert atmosphere. Firstly a solution of $[\text{Cu}(\text{NCMe})_4]\text{PF}_6$ in 15 ml of neat dichloromethane is added. Consequently, the flask is cooled down to -78 °C with a dry ice/acetone bath. Under stirring a solution of the xantphos-type ligand in 15 ml of neat dichloromethane is added dropwise to the reaction. The clear solution is then stirred for 2 hours at lowered temperature. Next, a solution of neocuproine (dmphen) in 20 mL neat dichloromethane is added dropwise into the solution under stirring and the reaction is left stirring for 2 hours. After letting the flask heat up to ambient temperature again the solvent is removed from the flask under vacuum. The resulting solid is dissolved again in 7 mL of dichloromethane and precipitated again by slowly adding 40 mL of diethyl ether. Further steps were carried out under normal atmosphere. Consequently, the precipitate was filtered through a ND4 glass frit under the vacuum of a water stream pump and washed with diethyl ether. The purified product is then recrystallized by slow diffusion of diethyl ether into a saturated solution of the complex. The crystals were washed with neat pentane.

$[\text{Cu}(\text{neocuproine})(p\text{-CF}_3\text{-xantphos})]\text{PF}_6$ ([1] PF_6)

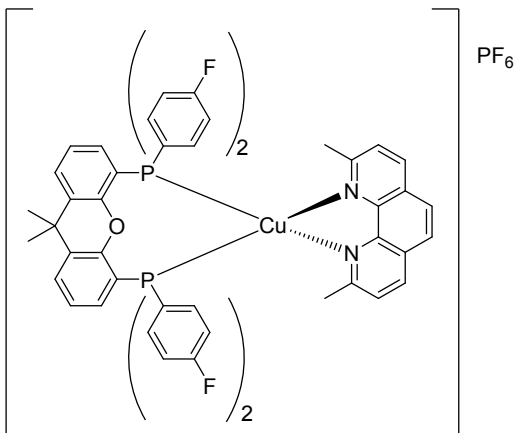
According to the general procedure using 26 mg (0.07 mmol) of $[\text{Cu}(\text{NCMe})_4]\text{PF}_6$, 50 mg (0.07 mmol) of $p\text{-CF}_3\text{-xantphos}$ and 15 mg (0.07 mmol) of neocuproine. After the work up, the desired product was obtained as orange crystals, mass 48.9 mg (yield 50 %). ^1H NMR (300 MHz, CD_2Cl_2 , 298 K): δ (ppm) = 8.35 (d, $^3\text{J}_{\text{H-H}} = 8.2$ Hz, 2H, CH), 7.87 (s, 2H, CH), 7.79 (dd, $^3\text{J}_{\text{H-H}} = 7.5$ Hz, $^4\text{J}_{\text{H-H}} = 1.3$ Hz, 2H, CH), 7.57 (d, $^3\text{J}_{\text{H-H}} = 8.2$ Hz, 2H, CH), 7.31 (d, $^3\text{J}_{\text{H-H}} = 8.1$ Hz, 8H, CH), 7.27 (t, $^3\text{J}_{\text{H-H}} = 7.6$ Hz, 2H, CH), 7.2-7.1 (m, 8H, CH), 6.89-6.80 (m, 10H, CH), 2.26 (s, 6H, CH_3), 1.79 (s, 6H, CH_3). $^{13}\text{C}-\{\text{H}\}$ NMR (75 MHz, CD_2Cl_2 , 298 K): δ (ppm) = 159.5 (s, Cq), 155.0 (t, $^1\text{J}_{\text{P-C}} = 6.2$ Hz, Cq), 143.9 (s, Cq), 139.1 (s, Cq), 135.6 (t, $^1\text{J}_{\text{P-C}} = 15$ Hz, Cq), 134.7 (t, $^3\text{J}_{\text{P-C}} = 2.0$ Hz, Cq), 133.4 (t, $^2\text{J}_{\text{P-C}} = 8.0$ Hz, CH), 132.4 (q, $^2\text{J}_{\text{F-C}} = 32.8$ Hz, Cq), 129.6 (s, CH), 128.7 (s, CH), 128.4 (s, Cq), 126.7 (s, CH), 126.4 (t, $^3\text{J}_{\text{P-C}} = 2.0$ Hz, CH), 126.2 (s, CH), 126.1 (s, CH), 123.8 (q, $^1\text{J}_{\text{F-C}} = 274.8$ Hz, Cq), 118.4 (t, $^2\text{J}_{\text{P-C}}$)



$C = 13.9$ Hz, Cq), 36.6 (s, Cq), 29.1 (s, CH₃), 26.4 (s, CH₃). ³¹P-{¹H} NMR (121 MHz, CD₂Cl₂, 298 K): δ (ppm) = -12.43 (s, P(Ph *p*-CF₃)), -144.4 (sept, ¹JF-P = 712.7 Hz, PF₆). ¹⁹F-{¹H} NMR (282 MHz, CD₂Cl₂, 298 K): δ (ppm) = -63.5 (s), -72.0 (s), -74.5 (s). HRMS ESI⁺ [M-PF₆]⁺: 1121.1733.

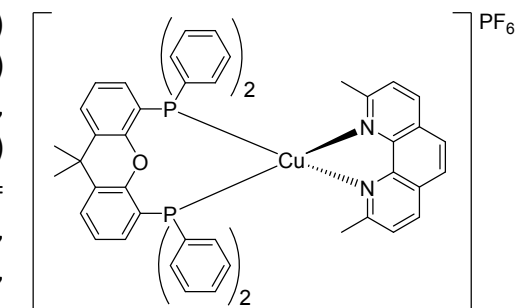
[Cu(neocuproine)(*p*-F-xantphos)]PF₆ ([2]PF₆)

According to the general procedure using 56 mg (0.14 mmol) of [Cu(NCMe)₄]PF₆, 100 mg (0.14 mmol) of *p*-F-xantphos and 29 mg (0.14 mmol) of neocuproine. After the work up, the desired product was obtained as orange crystals, mass 105.6 mg (yield 70 %). ¹H NMR (300 MHz, CD₂Cl₂, 298 K): δ (ppm) = 8.37 (d, ³JH-H = 8.3 Hz, 2H, CH), 7.91 (s, 2H, CH), 7.72 (dd, ³JH-H = 7.8 Hz, ⁴JH-H = 1.3 Hz, 2H, CH), 7.56 (d, ³JH-H = 8.3 Hz, 2H, CH), 7.23 (t, ³JH-H = 7.8 Hz, 2H, CH), 7.05-6.95 (m, 8H, CH), 6.83-6.73 (m, 10H, CH), 2.24 (s, 6H, CH₃), 1.77 (s, 6H, CH₃). ¹³C-{¹H} NMR (100 MHz, CD₂Cl₂, 298 K): δ (ppm) = 164.5 (d, ¹JF-C = 252.2 Hz, Cq), 159.6 (s, Cq), 155.6 (t, ¹JPC = 6.5 Hz, Cq), 144.0 (s, Cq), 138.8 (s, CH), 135.9 (m, CH), 134.9 (s, Cq), 130.9 (s, CH), 128.7 (s, CH), 127.6 (td, ¹JPC = 17.2 Hz, ⁴JF-C = 3.1 Hz, Cq), 126.5 (s, CH), 126.4 (t, ³JPC = 2.1 Hz, CH), 126.2 (s, CH), 121.8 (t, ²JPC = 12.9 Hz, Cq), 116.8 (dt, ³JF-C = 21.4 Hz, ²JPC = 4.9 Hz, CH), 36.9 (s, Cq), 28.9 (s, CH₃), 27.9 (s, CH₃). ³¹P-{¹H} NMR (121 MHz, CD₂Cl₂, 298 K): δ (ppm) = -13.75 (s, P(Ph *p*-F)₂), -144.29 (sept, ¹JF-P = 717.6 Hz; PF₆). ¹⁹F-{¹H} NMR (282 MHz, CD₂Cl₂, 298 K): δ (ppm) = -72.11 (s), -76.41 (s), -110.06 (s). HRMS ESI⁺ [M-PF₆]⁺: Not available due to sample degradation.



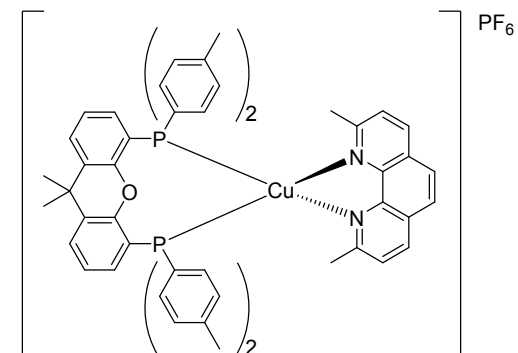
[Cu(neocuproine)(xantphos)]PF₆ ([3]PF₆)

According to the general procedure using 520 mg (1.4 mmol) [Cu(NCMe)₄]PF₆, 809 mg (1.4 mmol) of xantphos and 291 mg (1.4 mmol) neocuproine. The desired product was obtained as yellow crystals, mass 1.0618 g (yield 76 %). ¹H NMR (300 MHz, CD₂Cl₂, 298 K): δ (ppm) = 8.30 (d, ³JH-H = 8.26 Hz, 2H, CH), 7.82 (s, 2H, CH), 7.70 (dd, ³JH-H = 7.76 Hz, ⁴JH-H = 1.56 Hz, 2H, CH), 7.51 (d, ³JH-H = 8.38 Hz, 2H, CH), 7.29-7.18 (m, 6H, CH), 7.11-6.99 (m, 16H, CH), 6.96-6.89 (m, 2H, CH), 2.28 (s, 6H, CH₃), 1.76 (s, 6H, CH₃). ¹³C-{¹H} NMR (75 MHz, CD₂Cl₂, 298 K): δ (ppm) = 159.6 (s, Cq), 156.0 (t, ¹JPC = 6.8 Hz, CH), 143.8 (s, Cq), 138.6 (s, CH), 134.8 (s, Cq), 133.9 (t, ²JPC = 7.8 Hz, CH), 132.4 (t, ¹JPC = 16.2 Hz, Cq), 131.3 (s, CH), 130.8 (s, CH), 129.5 (t, ³JPC = 4.4 Hz, CH), 128.7 (s, Cq), 128.5 (s, CH), 126.8 (s, CH), 126.2 (s, CH), 126.1 (s, CH), 122.5 (s, Cq), 29.2 (s, CH₃), 28.0 (s, CH₃). ³¹P-{¹H} NMR (121 MHz, CD₂Cl₂, 298 K): δ (ppm) = -12.46 (s, P(Ph *p*-H)), -144.51 (sept, ¹JF-P = 703.9 Hz, PF₆). ¹⁹F-{¹H} NMR (282 MHz, CD₂Cl₂, 298 K): δ = -72.2 (s), -74.4 (s). HRMS ESI⁺ [M-PF₆]⁺: 849.2234. HRMS ESI⁺ [M-PF₆]⁺: 905.2836.



[Cu(neocuproine)(*p*-Me-xantphos)]PF₆ ([4]PF₆)

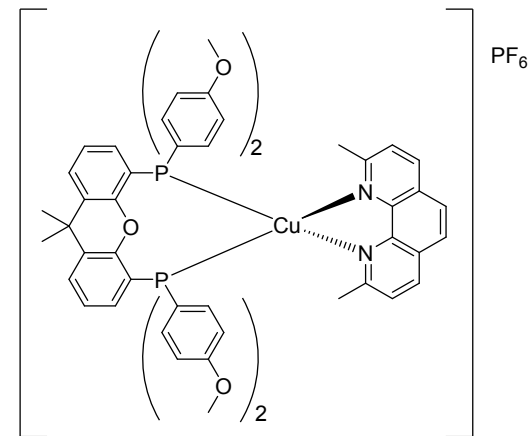
According to the general procedure using 56 mg (0.14 mmol) of [Cu(NCMe)₄]PF₆, 100 mg (0.14 mmol) of *p*-Me-xantphos and 29 mg (0.14 mmol) of neocuproine. After the work up, the desired product was obtained as orange crystals, mass 113.8 mg (yield 70 %). ¹H NMR (300 MHz, CD₂Cl₂, 298 K): δ (ppm) = 8.27 (d, ³JH-H = 8.16 Hz, 2H, CH), 7.82 (s, 2H, CH), 7.66 (dd, ³JH-H = 7.87 Hz, ⁴JH-H = 1.5 Hz, 2H, CH), 7.48 (d, ³JH-H = 8.2 Hz, 2H, CH), 7.25-7.15 (m, 2H, CH), 6.95-6.85 (m, 10H, CH), 6.85-6.78 (m, 8H, CH), 2.25 (s, 18H, CH₃), 1.75 (s, 6H, CH₃).



$^{13}\text{C}-\{\text{H}\}$ NMR (100 MHz, CD_2Cl_2 , 298 K): δ (ppm) = 159.5 (s, Cq), 155.9 (t, $^1\text{JPC} = 6.6$ Hz, Cq), 143.3 (s, Cq), 140.5 (s, Cq), 137.6 (s, CH), 134.2 (s, Cq), 133.4 (t, $^2\text{JPC} = 8.2$ Hz, 129.9 (t, $^3\text{JPC} = 4.6$ Hz, CH), 128.4 (t, $^1\text{JPC} = 17.9$ Hz, Cq), 128.0 (s, Cq), 127.9 (s, CH), 126.4 (s, CH), 122.6 (t, $^2\text{JPC} = 12.8$ Hz, Cq), 36.5 (s, Cq), 29.1 (s, CH_3), 27.4 (s, CH_3), 21.2 (s, CH_3). $^{31}\text{P}-\{\text{H}\}$ NMR (121 MHz, CD_2Cl_2 , 298 K): δ (ppm) = -13.52 (s, P(*p*-Me Ph)₂), -144.5 (sept, $^1\text{JFP} = 713.6$ Hz). $^{19}\text{F}-\{\text{H}\}$ NMR (282 MHz, CD_2Cl_2 , 298 K): δ (ppm) = -72.34 (s), -74.84 (s).

[Cu(neocuproine)(*p*-OMe xantphos)]PF₆ ([5]PF₆)

According to the general procedure using 52 mg (0.14 mmol) of [Cu(NCMe)₄]PF₆, 100 mg (0.14 mmol) of *p*-OMe-xantphos and 29 mg (0.14 mmol) of neocuproine. After the work up, the desired product was obtained as orange crystals, mass 87 mg (yield 56 %). ^1H NMR (300 MHz, CDCl_3 , 298 K): δ (ppm) = 8.35 (d, $^3\text{JHH} = 8.20$ Hz, 2H, CH), 7.87 (s, 2H, CH), 7.60 (dd, $^3\text{JHH} = 7.67$ Hz, $^4\text{JHH} = 1.35$ Hz, 2H, CH), 7.51 (d, $^3\text{JHH} = 8.49$ Hz, 2H, CH), 7.16 (t, $^3\text{JHH} = 7.79$ Hz, 2H, CH), 6.94-6.86 (m, 8H, CH), 6.84-6.78 (m, 2H, CH), 6.52-6.48 (m, 8H, CH), 3.72 (s, 12H, OCH₃), 2.21 (s, 6H, CH₃), 1.73 (s, 6H, CH₃). $^{13}\text{C}-\{\text{H}\}$ NMR (75 MHz, CDCl_3 , 298 K): δ (ppm) = 160.3 (s, Cq), 159.7 (s, Cq), 142.4 (s, Cq), 154.8 (s, Cq), 143.1 (s, Cq), 137.9 (s, CH), 134.6 (t, $^3\text{JPC} = 8.5$ Hz, CH), 134.0 (s, Cq), 130.5 (s, CH), 128.1 (s, Cq), 127.5 (s, CH), 126.6 (s, CH), 122.9 (t, $^1\text{JPC} = 12.0$ Hz, Cq), 122.3 (t, $^1\text{JPC} = 19.0$ Hz, Cq), 113.8 (t, $^2\text{JPC} = 4.6$ Hz, CH), 54.0 (s, OCH₃), 35.8 (s, Cq), 28.4 (s, CH₃), 27.9 (s, CH₃). $^{31}\text{P}-\{\text{H}\}$ NMR (121 MHz, CD_2Cl_2 , 298 K): δ (ppm) = -14.09 (s, P(Ph *p*-H)), -144.46 (sept, $^1\text{JFP} = 712.7$ Hz, PF₆). $^{19}\text{F}-\{\text{H}\}$ NMR (282 MHz, CD_2Cl_2 , 298 K): δ (ppm) = -72.4 (s), -75.3 (s). Crystal structure in Figure S4.



2. *In-situ* synthesis of photocatalyst [3]PF₆

To [Cu(NCMe)₄]PF₆ (0.001 mmol, 3 mol%) a solution of Xantphos (0.001 mmol, 3 mol%) in 0.5 mL MeNO₂ was added, after 1 min of rigorous stirring, a solution of Neocuproine (0.001 mmol, 3 mol%) in 0.5 mL MeNO₂ was added to the reaction dropwise, and the reaction was left stirring for 5 min, the quality of in situ generated photocatalyst is confirmed by NMR after the removal of solvent under vacuum and use CD_2Cl_2 as solvent.

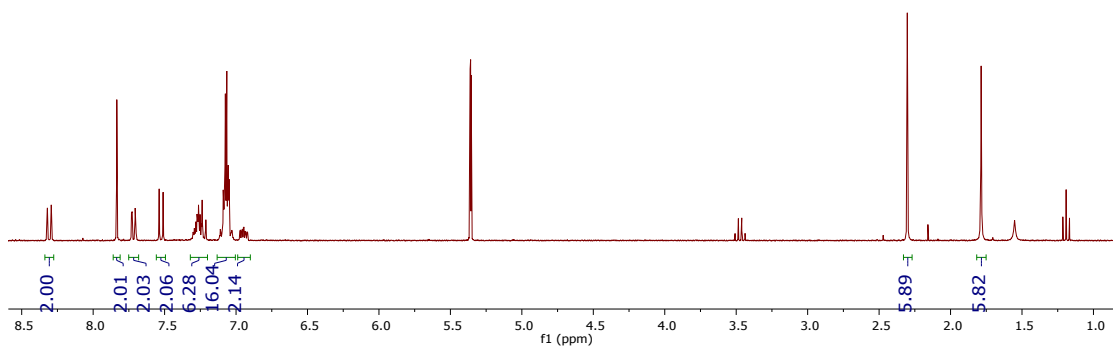


Figure S1: ^1H NMR (CD_2Cl_2 , 300 MHz, 298K) of the *in situ*-generated photocatalyst [3]PF₆

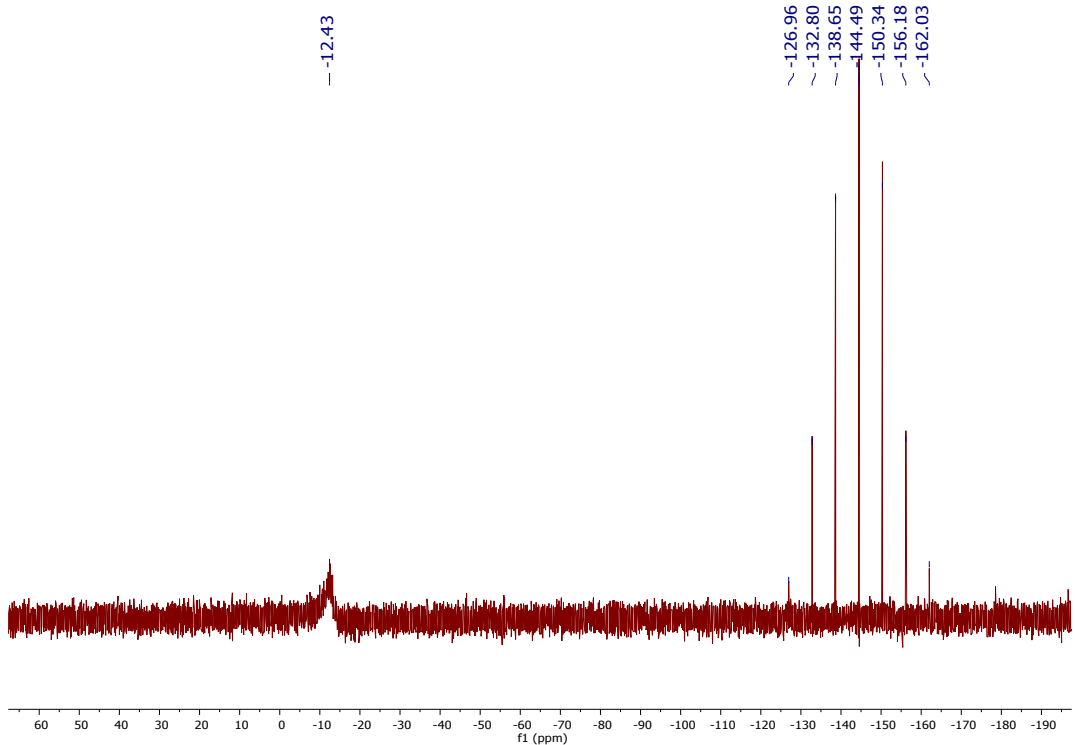


Figure S2: ^{31}P NMR (CD_2Cl_2 , 300 MHz, 298K) of the *in situ*-generated photocatalyst $[\mathbf{3}]\text{PF}_6$

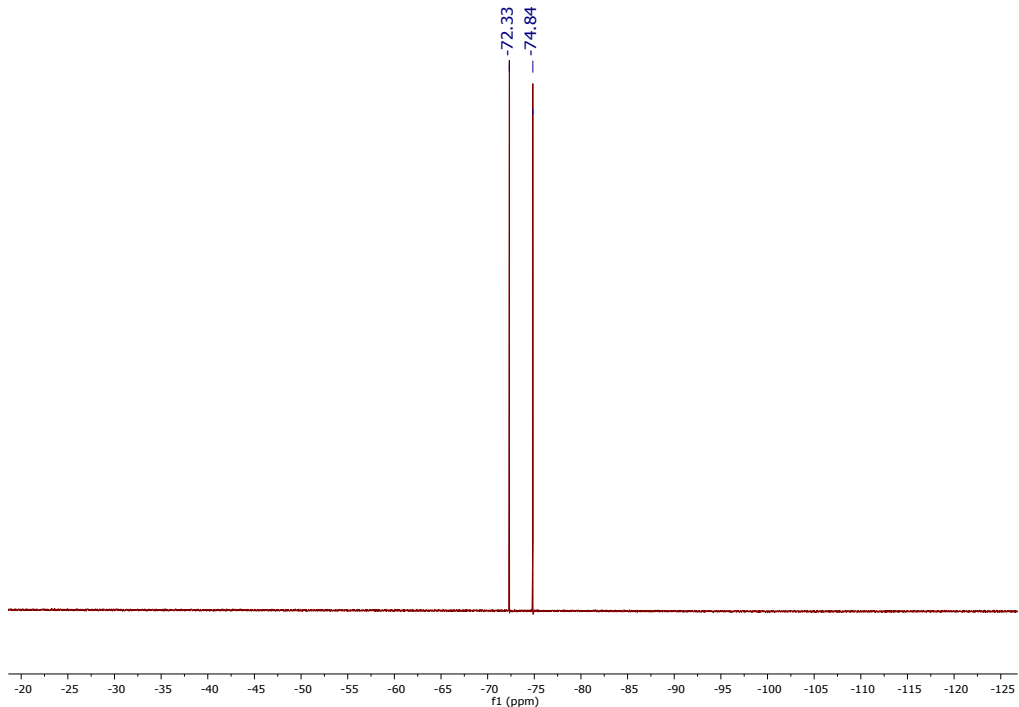


Figure S3: ^{19}F NMR (CD_2Cl_2 , 300 MHz, 298K) of the *in situ*-generated photocatalyst $[\mathbf{3}]\text{PF}_6$

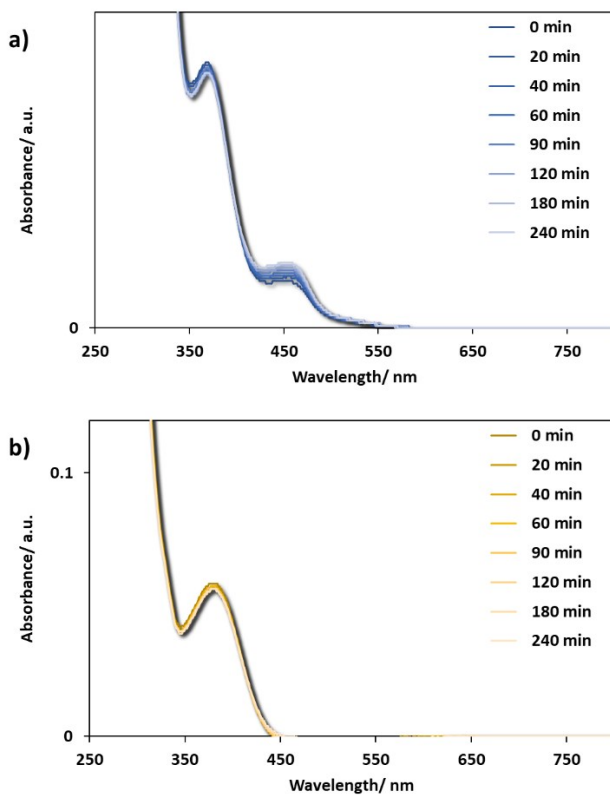


Figure S4: Photostability study monitored by UV-Vis absorption of (a) **1** and (b) **3** in MeCN under inert atmosphere (420 nm blue LED light). The growth of the band at 450 nm is indicative of the presence of $[\text{Cu}(\text{dmphen})_2]^+$.

3. X-Ray Diffraction

Crystals of **1** and **5** were obtained by slow diffusion of diethyl ether into a solution of the compound dissolved in dichloromethane. X-ray diffraction data for **1** were collected at 150 K on a Bruker Apex-II CCD diffractometer, and data for **6** were collected at 160 K on a STOE IPDS II diffractometer. The structures were solved by direct (SHELXS-97)⁴ or dual-space (SHELXT-2018/2)³⁰ methods and refined by full-matrix least-squares procedures on F^2 (SHELXL-2014/7 and -2018/3).⁵ Mercury⁶ was used for graphical representations. The structure of **1** showed poorly ordered, partial solvent molecules residing in channels running along the crystallographic a -axis. This disordered electron density was treated using the SQUEEZE³¹ routine implemented in PLATON.³² The solvent CHCl_3 molecule in **6** showed rotational disorder about one C–Cl bond, resulting in major and minor positions for the other two Cl atoms with occupancies of 0.621(9) and 0.379(9). Restraints to bond distances and thermal motion were required. CCDC 1979865 and 1950442 contains the supplementary crystallographic data for this paper. These data are provided free of charge by the joint Cambridge Crystallographic Data Centre and Fachinformationszentrum Karlsruhe Access Structures service www.ccdc.cam.ac.uk/structures.

Crystal data [**1**, Figure S4 (top)]: $\text{C}_{57}\text{H}_{40}\text{CuF}_{12}\text{N}_2\text{OP}_3$, $M = 1267.36$, monoclinic, space group $P2_1/n$, $a = 11.44340(10)$, $b = 20.2661(2)$, $c = 27.9804(4)$ Å, $\beta = 99.8050(10)^\circ$, $V = 6394.23(13)$ Å³, $T = 150(2)$ K, $Z = 4$, 99275 reflections measured, 11910 independent reflections ($R_{\text{int}} = 0.0328$), final R values [$I > 2\sigma(I)$]: $R_1 = 0.0786$, $wR_2 = 0.1611$, final R values (all data): $R_1 = 0.0798$, $wR_2 = 0.1611$, 743 parameters.

Crystal data [**5**, Figure S4 (bottom)]: $\text{C}_{58}\text{H}_{53}\text{Cl}_3\text{CuF}_6\text{N}_2\text{O}_5\text{P}_3$, $M = 1234.82$, monoclinic, space group $C2/c$, $a = 35.7359(9)$, $b = 12.1275(2)$, $c = 27.9938(7)$ Å, $\beta = 112.354(2)^\circ$, $V = 11220.4(5)$ Å³, $T = 160(2)$ K, $Z = 8$, 96521 reflections measured, 13528 independent reflections ($R_{\text{int}} = 0.0350$), final R values ($I > 2\sigma(I)$): $R_1 = 0.0432$, $wR_2 = 0.1157$, final R values (all data): $R_1 = 0.0607$, $wR_2 = 0.1218$, 730 parameters, 22 restraints.

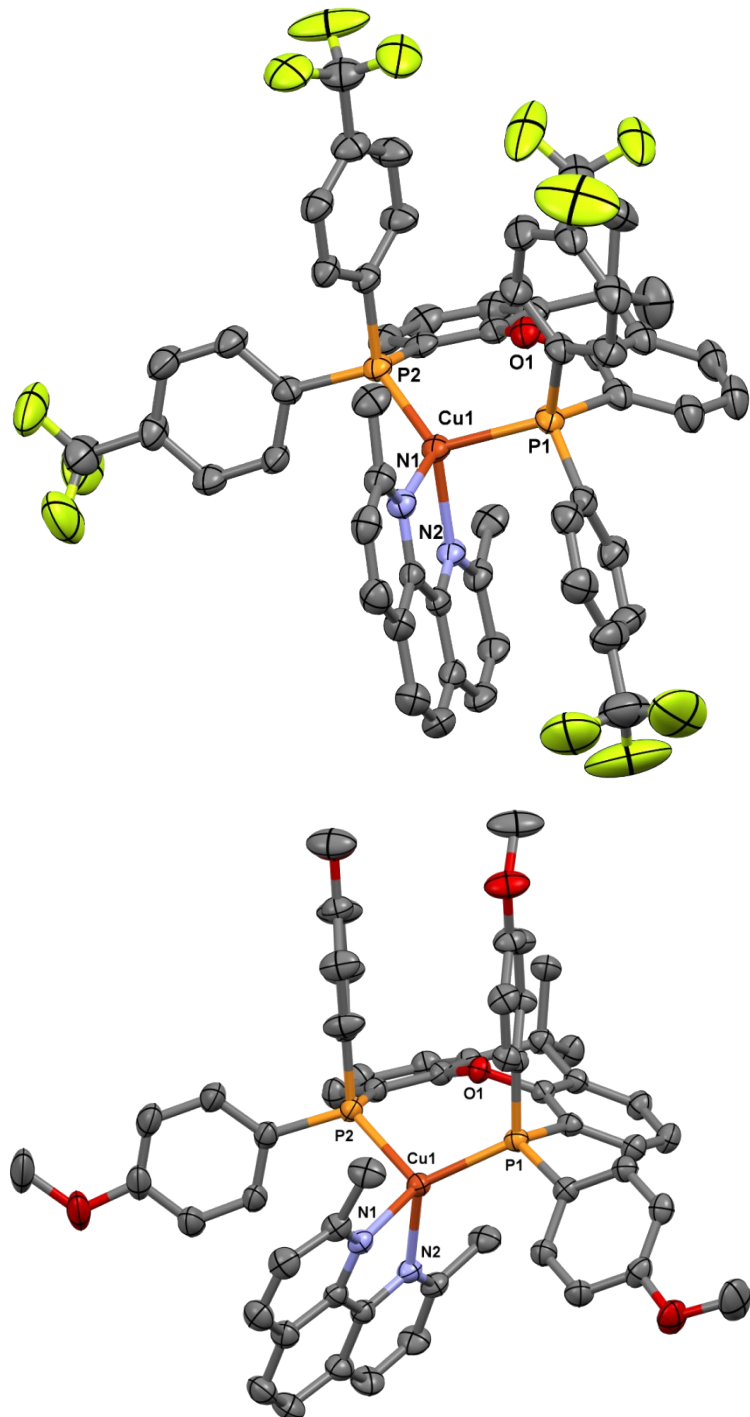


Figure S5: Molecular structures of **1** (top) and **5** (bottom). Hydrogen atoms, PF_6^- anion and solvent are omitted for clarity. Displacement ellipsoids correspond to 50% probability.

4. EPR Measurements

In situ EPR spectra were recorded at 20 °C using a quartz flat cell on X-band spectrometer (microwave frequency \approx 9.7 GHz; ELEXSYS 500-Bruker) with a microwave power of 6.9 mW, a modulation frequency of 100 kHz and modulation amplitude of 5G. The EPR optical resonator with a grid in the front side was used to irradiate the sample using 300 W Xe lamp (LOT Oriel). For the measurement, 3 mg of [5] PF_6^- were dissolved in 3 ml of degassed acetonitrile and transferred to the flat cell under argon.

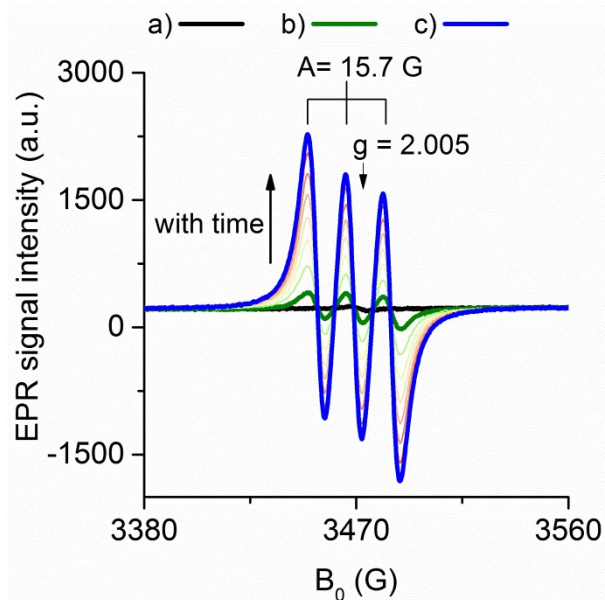


Figure S5: EPR spectrum of TEMPO obtained during photoirradiation of **[5]**PF₆ in CH₃CN solution in the presence of TEMP (10 μ L), a) under Ar (back line); b) after bubbling of O₂; c) after 8 min (blue line).

5. Photophysics

All samples were prepared in HPLC grade solvent with varying concentrations on the order of μ M. Absorption spectra were recorded at RT using a Shimadzu UV1800 double beam spectrophotometer. Molar absorptivity determination was verified by linear leastsquares fit of values obtained from at least five independent solutions at varying concentrations with absorbance ranging from 3.79×10^{-2} to 9.10×10^{-2} μ M.

The sample solutions for the room temperature emission measurements were prepared in HPLC grade dichloromethane and degassed using three freeze-pump-thaw cycles using an in-house designed quartz cuvette. Steady-state and time-resolved emission spectra were recorded at room temperature using a Gilden fluoroSENS fluorimeter. The samples were excited at 360 nm. Excited state lifetimes were measured by time correlated single photon counting (TCSPC) with an Edinburgh Instruments FLS980 fluorimeter using a pico-second pulsed diode laser (exciting at 378 nm) and PL emission was detected at the corresponding steady-state emission maximum for each complex. The PL decays were fitted to a single exponential decay function. In the case of multi-exponential fit the normalized pre-exponential factors are quoted. Emission quantum yields were determined using the optically dilute method.⁷ A stock solution was prepared and then four dilutions were prepared with absorbances of 0.01 to 0.1. The Beer-Lambert law was found to be linear at the concentrations of the solutions. The emission spectra were then measured after the solutions were rigorously degassed by three freeze-pump-thaw cycles prior to spectrum acquisition. For each sample, linearity between absorption and emission intensity was verified through linear regression analysis and additional measurements were acquired until the Pearson regression factor (R^2) for the linear fit of the data set surpassed 0.9. Individual relative quantum yield values were calculated for each solution and the values reported represent the slope value. The equation $\Phi_s = \Phi_r (A_r/A_s)(I_s/I_r)(n_s/n_r)^2$ was used to calculate the relative quantum yield of each of the sample, where Φ_r is the absolute quantum yield of the reference, n is the refractive index of the solvent, A is the absorbance at the excitation wavelength, and I is the integrated area under the corrected emission curve. The subscripts s and r refer to the sample and reference, respectively. An aerated solution of quinine sulfate in 0.5 M H₂SO₄ ($\Phi_r = 0.546$) was used as the external reference.⁸ Thin film PLQY measurements were performed using an integrating sphere in a Hammamatsu C9920-

O₂ system.⁹ Samples were excited by a xenon lamp coupled to a monochromator, which enabled selectivity of the excitation wavelength, chosen here to be 360 nm. The output was then fed into the integrating sphere via a fiber, exciting the sample. PL was collected with a multimode fibre and detected with a back-thinned CCD. The thin film PLQY were then measured in N₂ filled sphere. Film photophysics were performed in an Oxford instrument cryostat with a vacuum of less than 5×10^{-5} torr applied. Powder photophysics were performed in a home-made sample holder. All solid-state photophysics were measured using an Edinburgh Instruments FLS980 fluorimeter with a Xenon lamp (exciting at 360 nm) for steady-state measurements, and a pico-second pulsed diode laser (exciting at 378 nm) for TCSPC measurements, respectively.

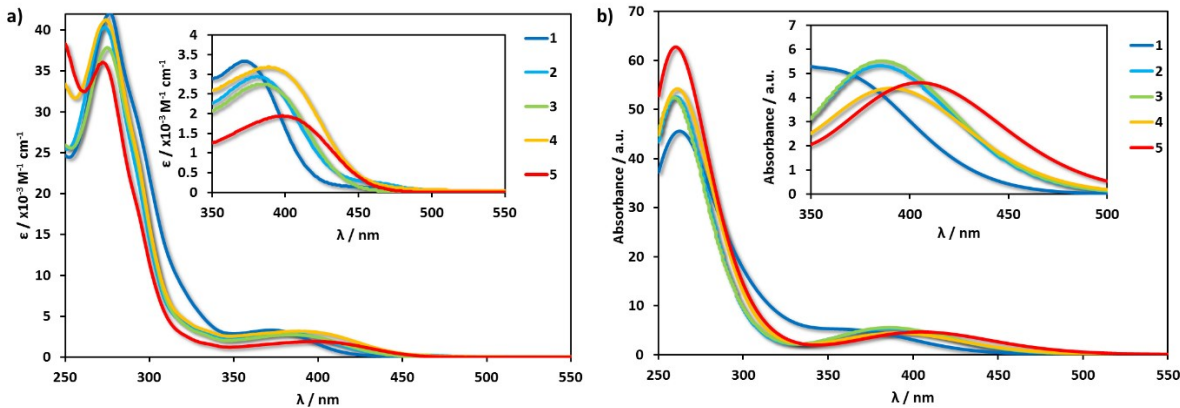


Figure S6: Absorption spectra of **1-5**. a) Measurements were carried out at 298 K in degassed HPLC DCM; b) Absorption spectra modelled from the TD-DFT (PBE0-D3/ECP1 level) results; Insets shows low energy absorption spectra illustrating the CT bands.

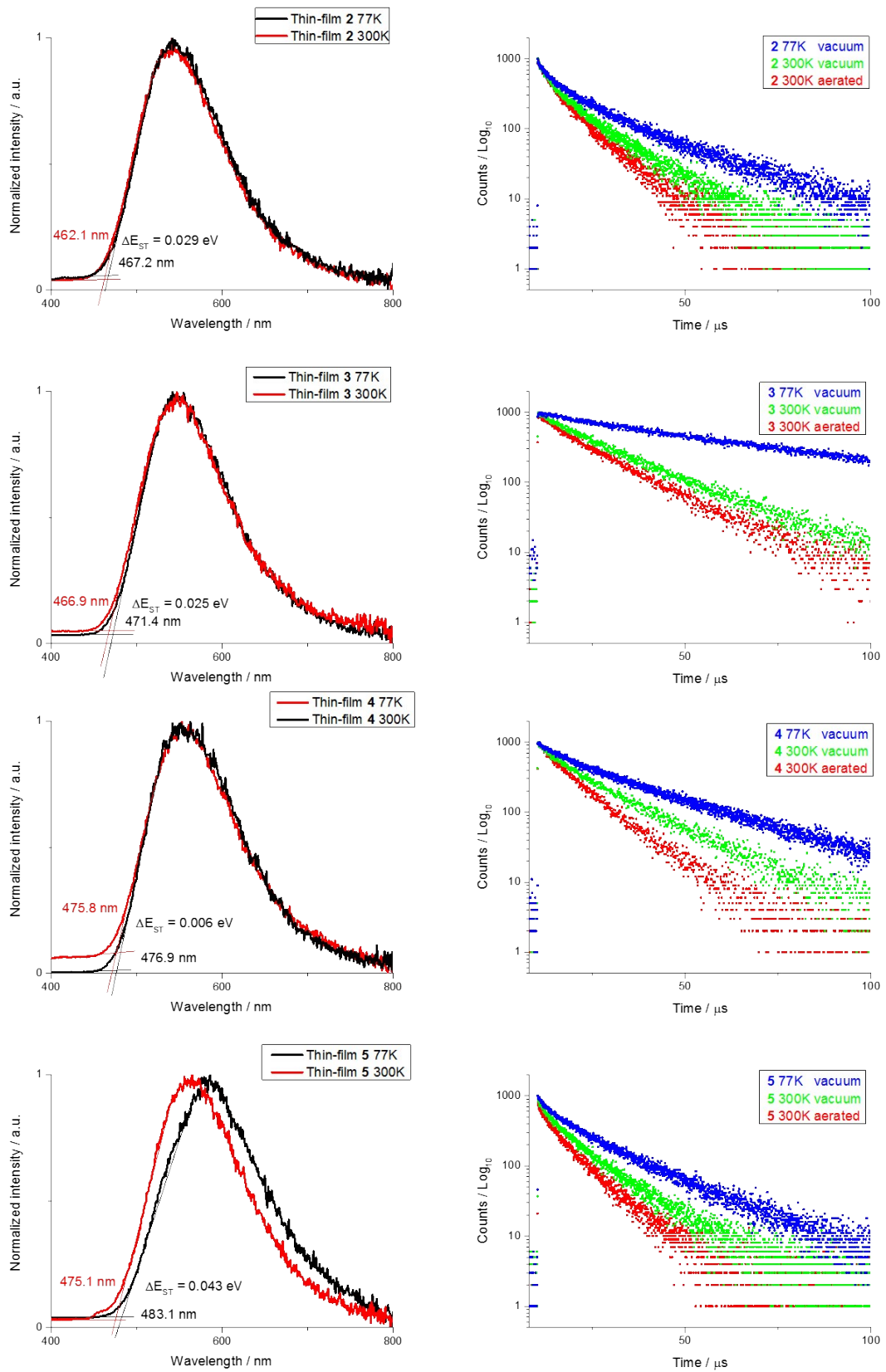


Figure S7: Neat film photophysics. Left, temperature dependent PL studies, and the ΔE_{ST} values measured from the onset emission energy at room temperature (S_1) and 77K (T_1). Right, excited state lifetime studies at different conditions (aerated, vacuum, and 77K) $\lambda_{\text{exc}} = 360 \text{ nm}$.

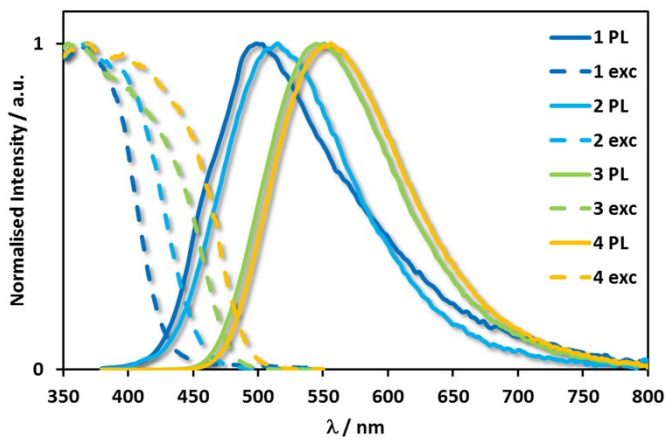


Figure S8: Powder photophysics $\lambda_{\text{exc}} = 360 \text{ nm}$.

Solid-state photophysics

Due to the CT nature of the excited state of $[\text{Cu}(\text{N}^{\text{N}})(\text{P}^{\text{P}})]^+$ complexes, they frequently show very small energy differences between their lowest triplet and singlet excited states (ΔE_{ST}), and have frequently been shown to be thermally activated delayed fluorescence (TADF) materials.⁶⁰ TADF compounds have received intense attention recently as emissive materials in electroluminescent devices as 100% of the electrogenerated excitons can be recruited through a thermally-promoted up-conversion of triplet excitons to singlet excitons via reverse intersystem crossing (RISC).⁶⁵ The powder and neat thin film photophysics of **1-4** were thus assessed and the data summarized in Table S1; the powder emission profiles are shown in Figure S8.⁴⁸

The electronic ligand effects on the solid-state emission properties in the neat film are consistent with those observed in solution (neat-film 526 nm for **1** and 557 nm for **5**; powder 498 nm for **1** and 561 nm for **5**). With electron-withdrawing groups present on the P^P ligand as in **1** and **2** the powder emission was blue-shifted compared to the neat film while with electron-donating groups present the powder emission was slightly red-shifted compared to the neat film. Interestingly, as observed in solution state, the energy of λ_{PL} for both, neat-film and powder samples display a strong Hammett correlation (Figures 11a, b).

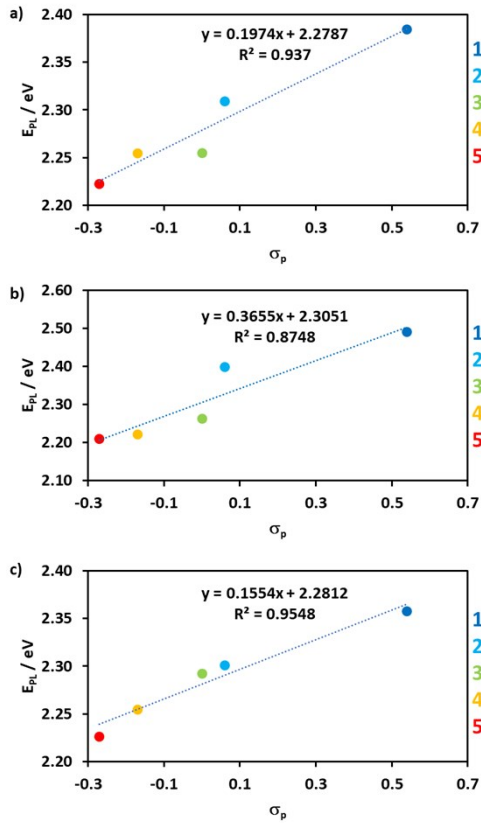


Figure S9 Hammett plots of the energy of λ_{PL} , a) solution samples, b) neat-film samples, c) powder samples.

In order to ascertain the nature of the emission, temperature-dependent time-resolved emission spectra were measured for complexes **2-5**; as **1** is very weakly emissive in the thin-film ($\Phi_{PL} < 1\%$) it was excluded in the temperature-dependent experiments. In each case, ΔE_{ST} was found to be very small with **5** showing the smallest ΔE_{ST} of only 6 meV while **5** having the largest ΔE_{ST} at 43 meV. These ΔE_{ST} values are sufficiently small to promote an efficient RISC process at ambient temperatures. Longer τ_{PL} were observed at 77 K compared to those at room temperature, indicating phosphorescence at low temperature. Excited state lifetimes are shorter in the presence of oxygen than under de-oxygenated conditions, corroborating that the emission of complexes **2-5** involves communication with triplet excited states at room temperature. Taken all together, it is clear that the emission in neat film at room temperature results from a TADF mechanism.

Both neat-film and powder samples of **1** are not very emissive with a Φ_{PL} less than 1 %, while complex **3** has the highest Φ_{PL} of 47 % in neat film and 38 % for powder under an N₂ atmosphere. The TADF complex [Cu(dmbpy)(xantphos)][BF₄], possessing the same P^AP ligand as **3**, shows a Φ_{PL} of 33% and an τ_{PL} of 15.1 μs in 5 wt% PMMA films.⁶⁶ Thus, complexes **3** and **4** represent potentially attractive emitters for electroluminescent devices as they show similar Φ_{PL} values but shorter τ_{PL} , indicating more efficient RISC. From DFT calculations on the T1 state it is shown that the electron density of the triplet state is almost exclusively based on the N^AN ligand and Cu centre (Figure 12). Emission to the ground state results from a mixed triplet metal-to-ligand charge transfer (³MLCT) and ligand-to-ligand charge transfer (³LLCT) transition. The broad, unstructured experimental emission band is consistent with the charge transfer nature of the emissive process

Table S1 Solid-state photophysics data^a.

Complex ^b	conditions	λ_{PL} /nm	CIE (x,y)	Φ_{PL} /% ^c	Φ_{PL} /% ^d	τ /μs	ΔE_{ST} /eV
1	Solution	520	0.29, 0.51		8.0	3.1 (100%) ^e	
	Powder	498	0.28, 0.42	<1		2.1 (9.3%), 20.7 (90.7%) ^f	
	Neat film	526	0.32, 0.46	<1	<1	0.1 (10.6%), 0.8 (46.0%) 3.2 (43.4%) ^e	
2	Solution	537	0.36, 0.55		11.8	3.4 (100%) ^e	
	Powder	517	0.29, 0.46	8.3		3.8 (22.0%), 14.4 (78.0%) ^f	
3	Neat film	539	0.35, 0.52	14.0	14.6	2.0 (13.3%), 12.2(86.7%) ^e	0.029
	Solution	550	0.39, 0.54		12.5	3.0 (100%) ^e	
	Powder	548	0.40, 0.54	37.7		15.6 (100%) ^f	
4	Neat film	541	0.37, 0.54	33.0	47.0	17.7 (100%) ^e	0.025
	Solution	550			9.3	6.2 (100%) ^e	
	Powder	558	0.42, 0.54	25.1		3.5 (10.5%), 15.1 (89.5%) ^f	
5	Neat-film	550	0.40, 0.54	26.0	36.0	14.2 (100%)	0.006
	Solution	558	0.42, 0.52		14.5	6.8 (100%) ^e	
	Powder	561	0.43, 0.53			0.1 (9.5%), 1.1 (49.3%), 4.1 (41.2%)	
5	Neat film	557	0.41,0.53	11.8	17.1	9.7 (100%) ^e	0.043

a) λ_{exc} = 360 nm for steady-state measurements and 379 nm for time-resolved measurements; b) [BF₄] was used as counteranion; c) under aerated conditions measured using an integrating sphere; d) under vacuum measured using an integrating sphere; e) excited-state lifetime under vacuum; f) excited-state lifetime under air.

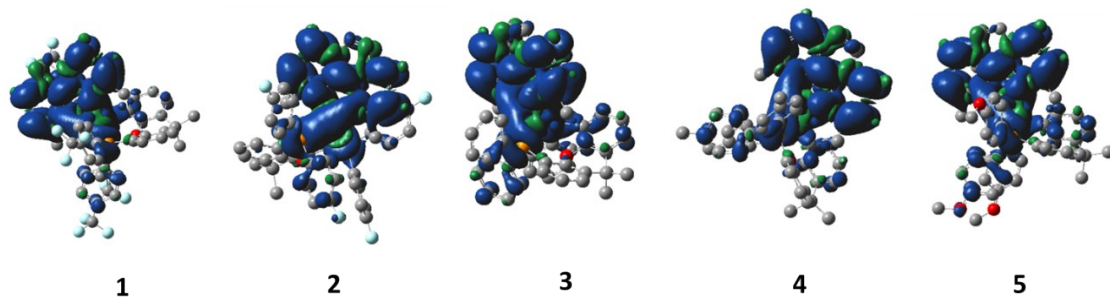


Figure S10 DFT calculated triplet spin density distributions of **1–5**, PBE0 level. Contours are at an isovalue of 0.02 a.u.

6. Electrochemistry

Cyclic voltammetry (CV) measurements were performed at room temperature with an electrochemical analyzer potentiostat model 620E from CH Instruments at a sweep rate of 50 mV/s. Differential pulse voltammetry (DPV) was conducted with an increment potential of 0.004 V and a pulse amplitude, width, and period of 50 mV, 0.05, and 0.5 s, respectively. Solutions for CV and DPV were prepared in MeCN/DCM and degassed with MeCN/DCM-saturated N₂ bubbling for about 10 min prior to scanning. Tetra(*n*-butyl)ammonium hexafluorophosphate (TBAPF₆; ca. 0.1 M in MeCN/DCM) was used as the supporting electrolyte. A silver wire was used as the pseudoreference electrode; a glassy-carbon electrode was used for the working electrode and a Pt wire was used as the counter electrode. The redox potentials are reported relative to a standard calomel electrode (SCE) electrode with a ferrocenium/ferrocene (Fc/Fc⁺) redox couple as an internal reference (0.38 V vs SCE for MeCN and 0.46 V vs SCE for DCM).^{10, 11}

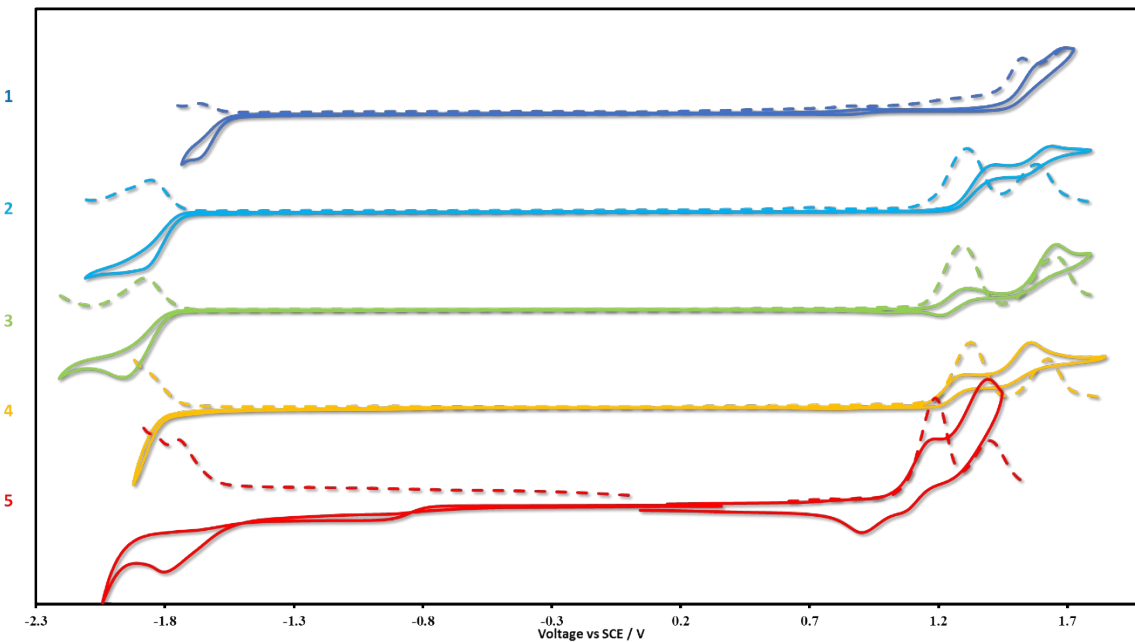


Figure S11: CV and DPV of **1-5** measured in degassed DCM with 0.1 M TBAPF₆ as the supporting electrolyte using a glassy carbon working electrode, a platinum wire counter electrode, a Ag/Ag⁺ pseudo-reference electrode and referenced vs. SCE using Fc/Fc⁺ as an internal standard (0.46 V in DCM).¹⁰ Scan rate: 50 mV s⁻¹.

Table S2 Ground and excited state electrochemical data of **1-5**

Complex	E _{ox} / V ^a	E _{red} / V ^a	ΔE _{redox} / V ^a	E _{opt} / V ^b	E [*] _{ox} / V ^c	E [*] _{red} / V ^c	E _{HOMO} / eV ^d	E _{LUMO} / eV ^d	E _{HOMO-LUMO} / eV
1	1.51	-1.74	3.25	2.86	-1.35	1.12	-5.93	-2.74	3.19
2	1.32	-1.96	3.28	2.65	-1.33	0.69	-5.74	-2.60	3.14
3	1.18	-2.03	3.21	2.72	-1.54	0.69	-5.61	-2.54	3.07
4	1.25	-1.67 ^f	2.92	2.66	-1.41	0.99	-5.63	-2.55	3.08
5	1.12	-1.71	2.92	2.63	-1.51	0.92	-5.55	-2.57	2.98

a) electrochemical measurements carried out in a degassed HPLC grade DCM with glassy carbon working electrode, Ag/Ag⁺ reference electrode and a platinum wire counter electrode. Fc/Fc⁺ was used as the internal standard and the data reported versus SCE (0.46 V vs SCE in DCM);¹⁵ b) optical gap inferred from the onset of the absorption of the MLCT band, defined as the energy at 10% relative intensity of the maximum on the low energy tail; c) excited state redox potentials calculated with equation E^{*}_{ox} = E_{ox} - E_{opt}, E^{*}_{red} = E_{red} + E_{opt};⁴ d) E_{HOMO} = -(E_[onset,ox vs. Fc⁺/Fc] + 4.8)(eV) E_{LUMO} = -(E_[onset,red vs. Fc⁺/Fc] + 4.8)(eV);³ e) the oxidation potential of second oxidation wave; f) reduction wave scanned in degassed acetonitrile solution since no reduction wave was observed in DCM solution.

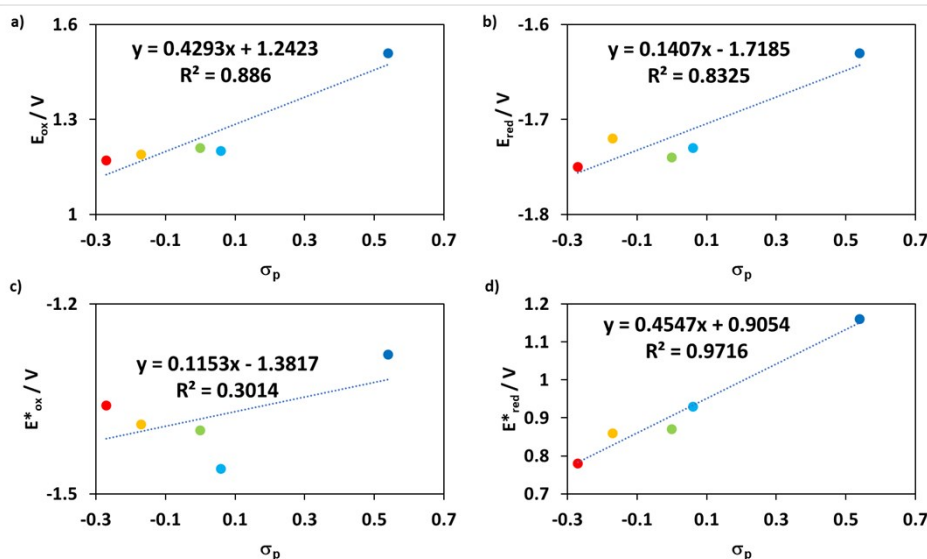


Figure S12: a) the Hammett plot of the oxidation potential; b) the Hammett plot of the reduction potential; c) the Hammett plot of the excited state oxidation potential; d) the Hammett plot of the excited state reduction potential.

7. Computational Details

Geometries were optimized in the gas phase at the PBE0-D3 level¹²⁻¹⁴ (including Grimme's dispersion correction¹⁵⁻¹⁷ with Becke-Johnson damping, a relativistic effective core potential on Cu and 6-31G* basis elsewhere (denoted ECP1).¹⁸ Frequency calculations were performed to ensure that the optimised structures were true minima on the potential energy surface. At this level, the structure of the parent complex **3** in the solid is well reproduced (see PBE0-D3 entry in Table S3). Energies were refined using a polarizable continuum model (PCM)¹⁹ with the parameters for dichloromethane as implemented in Gaussian 09²⁰, which was used for all calculations. Absorption energies were calculated using time-dependent DFT²¹ at the B3LYP^{22, 23}/ECP1 and PBE0/ECP1 levels (for complex **1** also at the CAM-B3LYP level),²⁴ together with the PCM with the parameters for dichloromethane. For compatibility with previous work from our group, we also optimised geometries at the B3LYP level in conjunction with the SBKJC effective core potential and its associated valence double-zeta basis for Cu and 6-31G** elsewhere,²⁵ together with the conductor-like PCM variant (CPCM) using the parameters of dichloromethane. These results are denoted B3LYP/SBKJC in the following.

Table S3: Mean Cu-ligand bond distances in complex **3** [in pm] optimised using various functionals (ECP1 basis); ***in bold italics***: mean absolute errors (MAE) [in pm].

Functional	Cu-N	Cu-P	<i>MAE</i>
B3LYP	219.3	236.6	<i>8.5</i>
PBE0	215.7	232.6	<i>3.5</i>
PBE0-D3	213.4	228.0	<i>1.5</i>
X-Ray ^a	210.9	227.6	-

^aCounterion tetrakis(3,5-bis(trifluoromethyl)phenyl)borate, CSD refode ARURB, from reference²⁶.

Using the PBE0-D3 optimised structure, the absorption spectra were calculated for the parent complex **3** at the TD-DFT level with B3LYP, CAM-B3LYP and PBE0 functionals. Somewhat surprisingly, CAM-B3LYP performs worst of all functionals, even though it was designed for correct long-range asymptotic behaviour, which should be beneficial for long-range charge-transfer bands (usually a challenge for TD-DFT). Both B3LYP and PBE0 reproduce experimental results with good accuracy. The intense $\pi-\pi^*$ band around 270 nm is slightly better represented by the B3LYP functional, whereas the PBE0 functional performs best for the CT band around 390 nm.

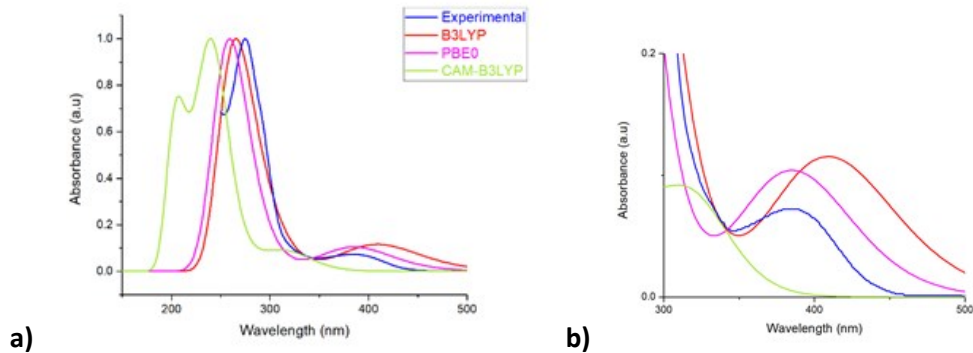


Figure S13: a) Overlay of computed and experimental (this work) absorption spectra of complex **4**; b) zoom into the region around 390 nm.

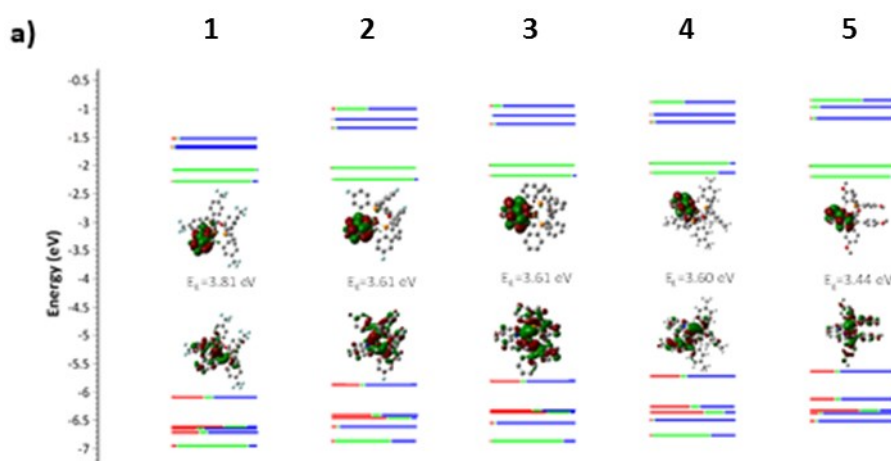
Table S4: TD-PBE0/ECP1 computed absorptions in complex **1**.^a

$\lambda_{\text{absorbance}} / \text{nm}$	Oscillator Strength f	Composition	Character
414.54	0.1047	HOMO -> LUMO (98%)	MLCT and LLCT
296.53	0.05	HOMO -> LUMO+4 (91%)	MLCT and $\pi \rightarrow \pi^*$
292.17	0.0604	HOMO-> LUMO+5 (92%)	MLCT and $\pi \rightarrow \pi^*$
267.87	0.0518	HOMO-5 -> LUMO+1 (38%); HOMO-8 -> LUMO+1 (26%)	$\pi \rightarrow \pi^*$
263.82	0.0529	HOMO-7 -> LUMO+1 (17%); HOMO-11 -> LUMO (16%); HOMO -> LUMO+10 (16%)	$\pi \rightarrow \pi^*$
263.60	0.0537	HOMO-6 -> LUMO+1 (33%); HOMO-13 -> LUMO (20%)	$\pi \rightarrow \pi^*$
262.43	0.1941	HOMO-14 -> LUMO (28%); HOMO-8 -> LUMO+1 (11%)	$\pi \rightarrow \pi^*$
259.44	0.0653	HOMO-3 -> LUMO+3 (56%)	$\pi \rightarrow \pi^*$

^aTransitions with oscillator strength > 0.05; colour coding of the main contributing fragments: red: Cu, green: phenanthroline, blue: Xantphos moieties.

Results with other functionals

In the main paper, (TD-)PBE0/ECP1(PCM) // PBE0-D3/ECP1 results are discussed. In the following, related graphical and tabular material is collected that has been obtained with different functionals. B3LYP/ECP1 denotes results at the (TD-)B3LYP/ECP1(PCM) // PBE0-D3/ECP1 level, B3LYP/SBKJC denotes results at the (TD-)B3LYP/SBKJC(CPCM) // B3LYP/SBKJC level.



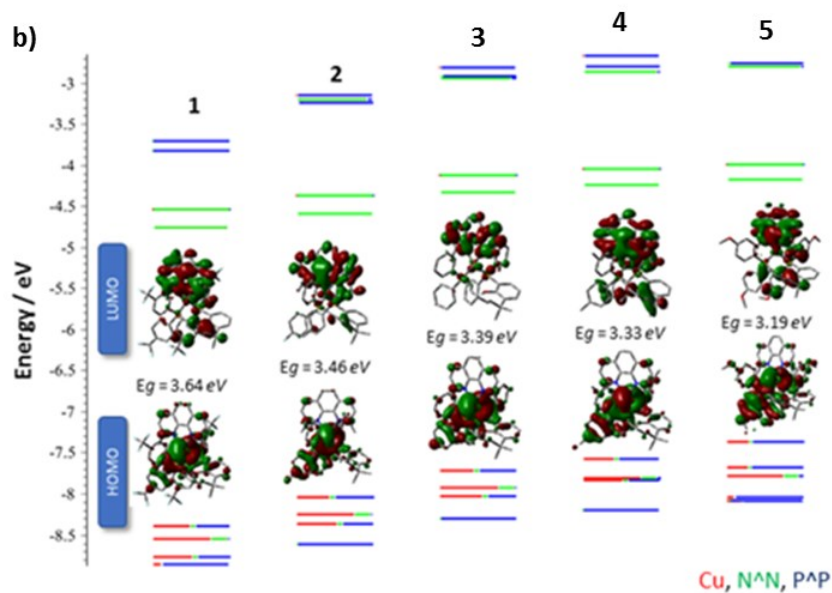


Figure S14: DFT calculations for **1-5**. Kohn-Sham energy diagram with electron density distribution of HOMO and LUMO shown. Red bars represent Cu orbitals, green bars represent orbitals on the N^{^N} ligand and the blue bars represent orbitals on the P^{^P} ligand. a) B3LYP/ECP1 level; b) B3LYP/SBKJC level

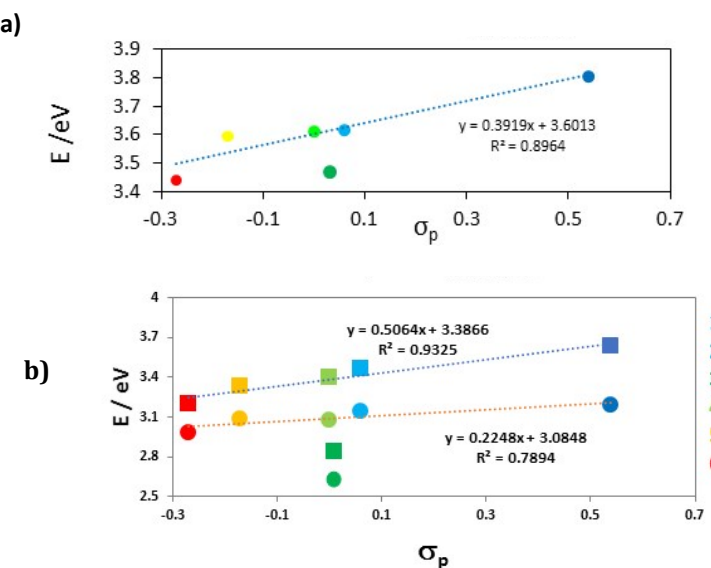


Figure S15: Hammett plots of HOMO-LUMO bandgap; a) B3LYP/ECP1 level, b) B3LYP/SBKJC level (squares), including gaps evaluated from electrochemistry (circles).

Table S5: Computed absorption data for the CT transition in complexes **1-5** from TD-B3LYP calculations.

Complex	$\lambda / \text{nm} (f)^a$	B3LYP/ECP1		B3LYP/SBKJC	
		Contributions		Contributions	
1	419 (0.077)	HOMO->LUMO (94%)		392 (0.146)	HOMO->LUMO (89%)
2	413 (0.100)	HOMO->LUMO (98%)		419 (0.146)	HOMO->LUMO (98%)
3	415 (0.105)	HOMO->LUMO (98%)		413 (0.148)	HOMO->LUMO (97%)
4	422 (0.075)	HOMO->LUMO (97%)		418 (0.146)	HOMO->LUMO (98%)
5	437 (0.090)	HOMO->LUMO (96%)		434 (0.132)	HOMO->LUMO (95%)

^aIn parentheses: oscillator strengths.

8. Photocatalysis

General procedure

A 10 mL Pyrex Schlenk tube equipped with a rubber septum and a magnetic stirring bar was charged with $[\text{Cu}(\text{NCMe})_4]\text{PF}_6$ (0.001 mmol, 3 mol%) and dissolved by 0.5 mL MeNO_2 , followed by a solution of Xantphos (0.001 mmol, 3 mol%) in 0.5 mL MeNO_2 after 1 min of rigorous stirring, a solution of Neocuproine (0.001 mmol, 3 mol%) in 0.5 mL MeNO_2 was added to the reaction dropwise, and the reaction was left stirring for 5 min to form the photocatalyst $[\text{Cu}(\text{dmphen})(\text{P}^{\wedge}\text{P})]\text{PF}_6$ (0.001 mmol, 3 mol%). Then 2-phenyl-1,2,3,4-tetrahydroisoquinoline (7 mg, 0.03 mmol), mesitylene (1.8 mg, 0.015 mmol) and nitromethane (1.5 mL) were added. A stream of oxygen was bubbled through the mixture for 5 min. The tube was provided with a balloon filled with oxygen and irradiated with a sapphire blue LED strip at ambient temperature ($24\text{-}26\text{ }^\circ\text{C}$, monitored by thermometer), emission wavelength centered at 453 nm. After irradiation, the solvent was removed under vacuum and the residue dissolved in deuterated chloroform for ^1H NMR analysis of the crude mixture. For kinetic profiles 0.1 mL samples were taken by syringe and

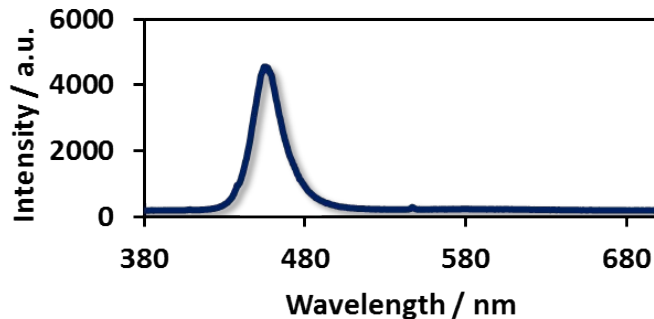


Figure S16: Set up for the photocatalytic experiments (left) and emission spectrum of blue LED irradiation source (right)

Screening of reaction conditions

Table S6: Condition screening for the aerobic photocatalyzed Aza-Henry reaction between **6** and nitromethane.^a

Entry	Cu^b	Neocuproine	Xantphos	O_2^c	Light ^d	Temperature ^e	Yield@18h ^f	
1^g	✓	✓		✓	✓	Ambient	78%	
2^h	✓	✓		✓	✓	Ambient	85%	
3	✓	✓		✓	X ⁱ	✓	Ambient	45%
4	✓	✓		✓	✓	X	Ambient	Trace
5	✓	✓		✓	✓	X	50 °C	Trace
6^j	✓	X		✓	✓	✓	Ambient	67%

7^k	✓	✓	X	✓	✓	Ambient	66%
8^l	X	✓	✓	✓	✓	Ambient	74%
9	X	X	X	✓	✓	Ambient	49%

a) conditions: **6** (0.03 mmol), Copper(I) photocatalyst (0.001 mmol, 3 mol%), MeNO₂ (3 mL), O₂ atmosphere (1 bar); b) [Cu(NCMe)₄][PF₆] made according to the literature²⁷ was used as copper precursor; c) Oxygen was bubbled for 5 min, and a balloon full of oxygen is used to maintain the oxygenated condition; d) 1 m long blue (450 nm) LED strip is used to irradiate the reactions; e) temperature measured during reactions, compressed air was used to maintain the ambient temperature (24–26 °C); f) GC and NMR yield obtained after 18 hours of crude reaction using Mesitylene as an external standard; g) in situ formed photocatalyst; h) premade photocatalyst [Cu(dmpphen)(Xantphos)][PF₆]; i) open to air without Oxygen bubbling; j) [Cu(NCMe)₄][PF₆] (0.001 mmol, 3 mol%), Xantphos (0.002 mmol, 6 mol%); k) [Cu(NCMe)₄][PF₆] (0.001 mmol, 3 mol%), Neocuproine (0.002 mmol, 6 mol%); l) Xantphos (0.001 mmol, 3 mol%) Neocuproine (0.001 mmol, 3 mol%).

9. Mechanistic studies:

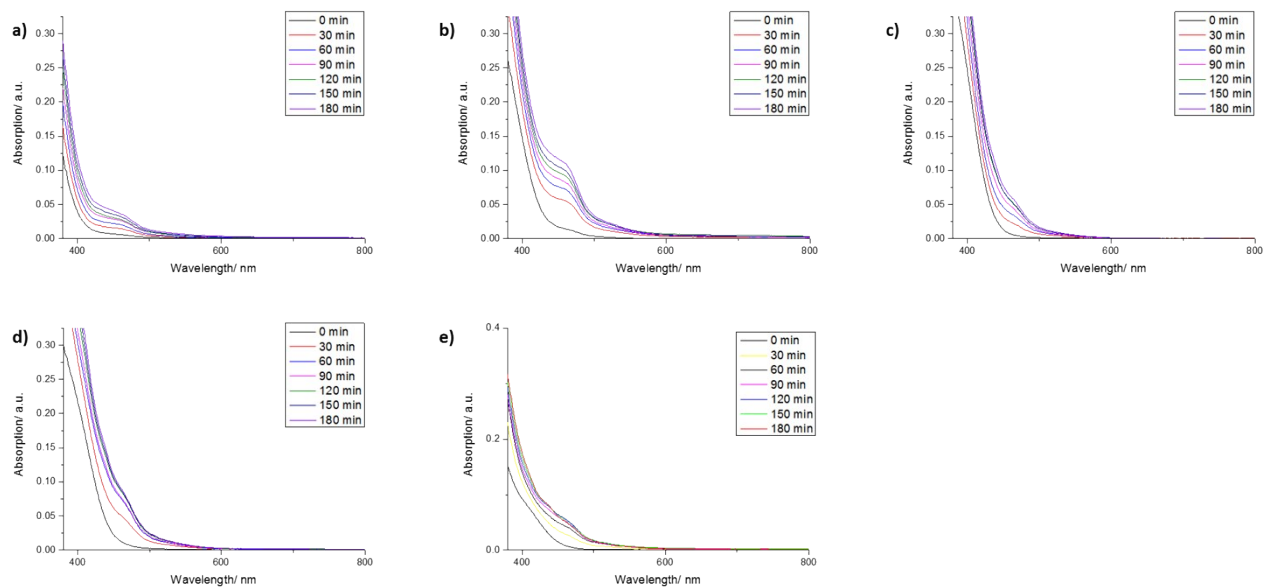


Figure S17: UV-Vis absorption spectra used to monitor the reactions under the adapted reaction condition for a) complex **1**, b) complex **2**, c) complex **3**, d) complex **4**, e) complex **5**, concentration of reactions was 1×10^{-5} M, stoichiometric amount of photocatalysts were used, the reactions were irradiated with 420 nm LED light.

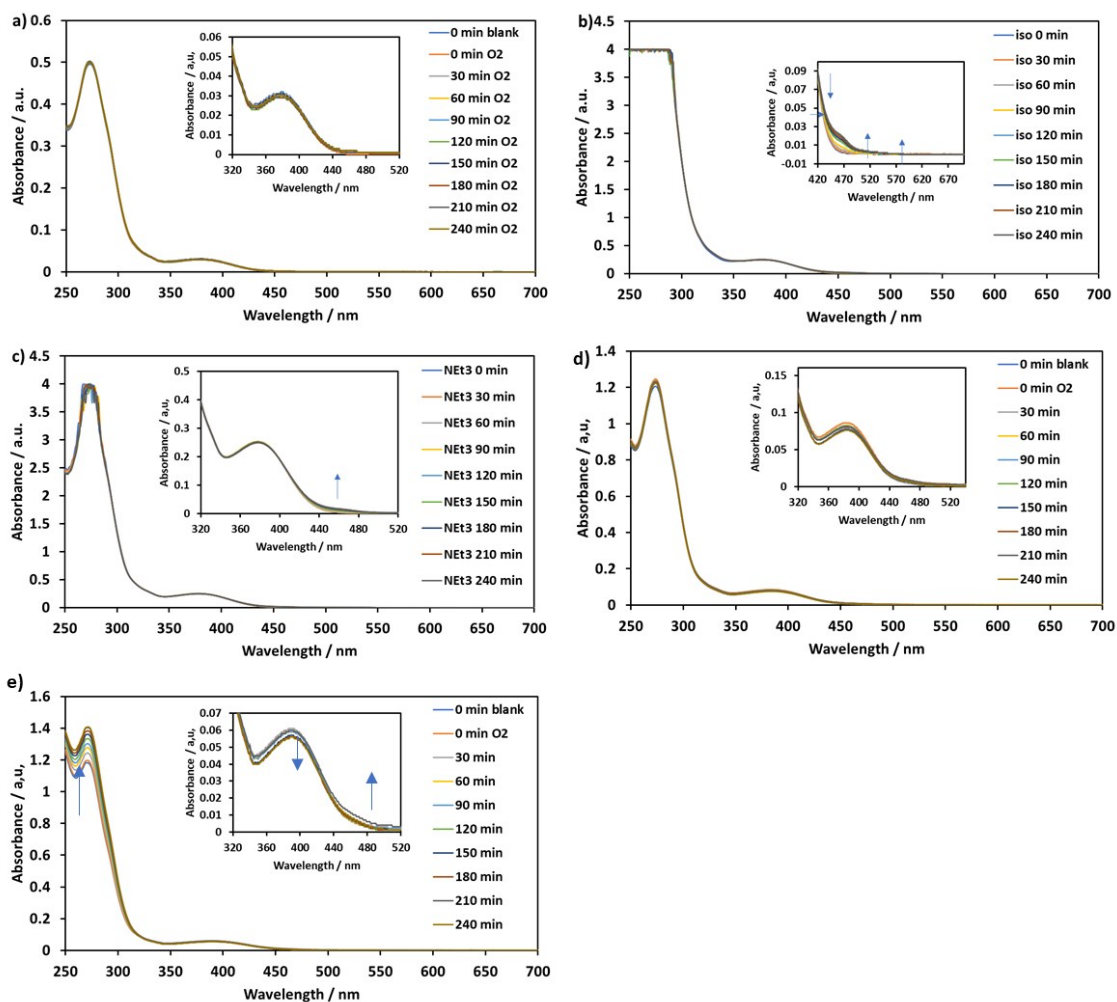


Figure S18: Absorption spectra of the MeCN solution of complex **3** and a) O_2 , b) **6**, c) NEt₃, d) complex **5** and O_2 , e) complex **5** and O_2 under 420 nm light irradiation using an LED array.

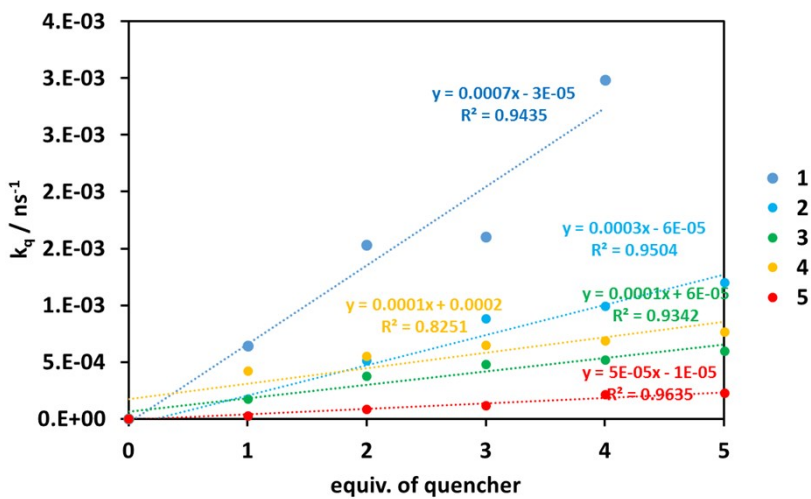


Figure S19: Stern-Volmer quenching experiments using triethylamine as quencher. Both copper complex and quencher solutions were degassed by three freeze-pump-thaw and refilled with Nitrogen. The emission profile of each sample was measured, and the quenching rate constant was calculated via the equation: $k_q = (I_0 - I)/\tau_0 I$ (I represents emission intensity, I_0 represents emission intensity without quencher, τ_0 represents excited state lifetime without quencher).

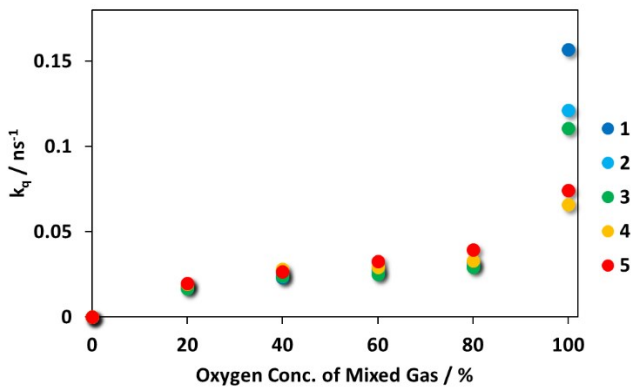


Figure S20: Stern-Volmer quenching experiments using O_2 as quencher. Both gas streams with different oxygen concentration in nitrogen were generated by a gas mixer, and 50 mL of HPLC grade acetonitrile was bubbled with corresponding pre-mixed gas for 10 mins before the stream was used to bubble the sample solution for 10 mins. Due to the different solubility of N_2 and O_2 , the concentration of O_2 in sample solutions is unknown, while the pure oxygen bubbled sample were used as the mimic of reaction conditions. The excited state lifetime of each sample was measured by TSCPC, and the quenching rate constant was calculated via equation: $k_q = 1/\tau - 1/\tau_0$ (τ_0 represents excited state lifetime without quencher, τ represents excited state lifetime with quencher).

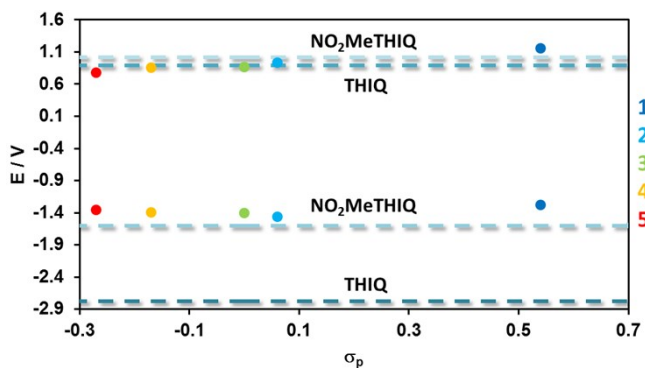


Figure S21: The redox potential of **6** and **7** (dashed line), and the E^*_{ox} and E^*_{red} of complexes **1-5**

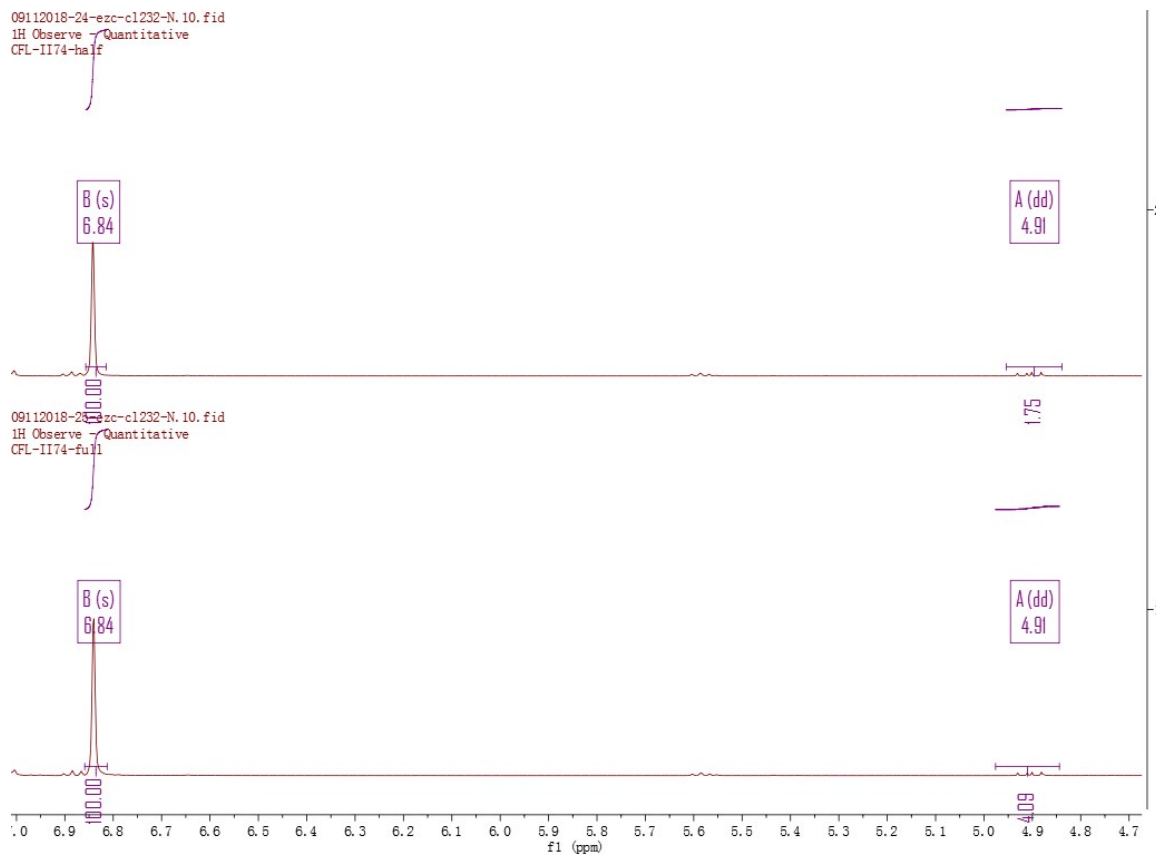


Figure S22: Two reactions with same stoichiometries of **3**, tetrahydroisoquinoline, Nitromethane were bubbled with O₂ for 10 mins before being irradiated with same blue LED strips while one of the LED strips is covered with aluminum foil.²⁸ To exclude other influencing factors, such as, adverse effects of prolonged reaction time, the reactions were radiated for 1 hour. After 1 hour the irradiation was stopped for both the reactions, and the reactions were carefully covered by aluminum foils to protect from sunlight/ambient light, internal standard mesitylene was injected to both mixtures, followed by vigorous shacking. The quantitative ¹H-NMR was used to analyze the result (relaxation delay 60 s), and the integration showed 4.09:1.75 (full power: half power) which supported the 1-photon excitation mechanism conjecture.

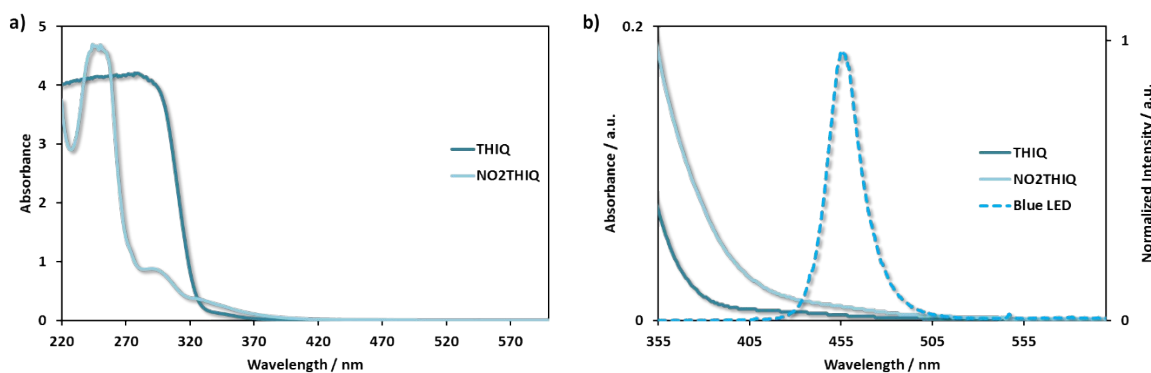


Figure S23: UV-Vis spectra of THIQ and NO₂THIQ in MeCN, a) 220-600 nm, b) 355-600 nm with the emission spectra of blue LED used in photoredox reactions.

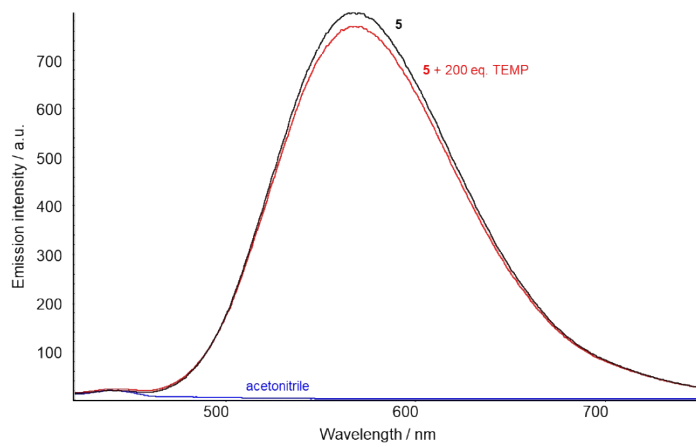


Figure S24: Steady-state emission spectra of **5** in acetonitrile in the presence (red) and absence (black) of TEMP (2,2,6,6-tetramethylpiperidine). The small differences in the emission intensity are within the experimental error. A Cary Eclipse Fluorescence spectrophotometer (Agilent Technologies) with an excitation wavelength of 390 nm, a slit width of 10 nm for excitation and of 20 nm for emission and an averaging time of 0.1 s was used. The studies were performed in a sealable 1x1 cm quartz glass cuvette. The oxygen amount was adjusted by addition of the corresponding amount of an O₂-saturated acetonitrile solution (2.6 mM O₂)²⁹ to the solution of **5**.

10. Comparison between BF₄⁻ and PF₆⁻

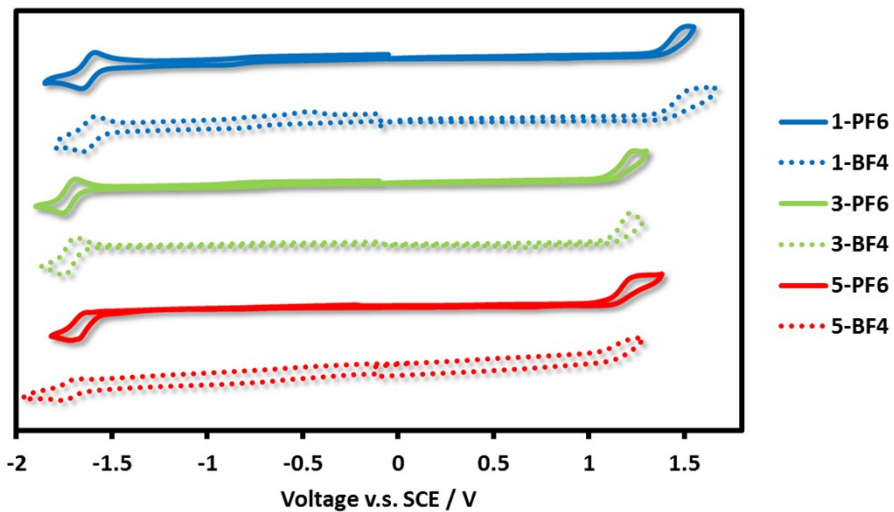


Figure S25: Cross comparison of CV in MeCN of complex **1**, **3**, **5**.

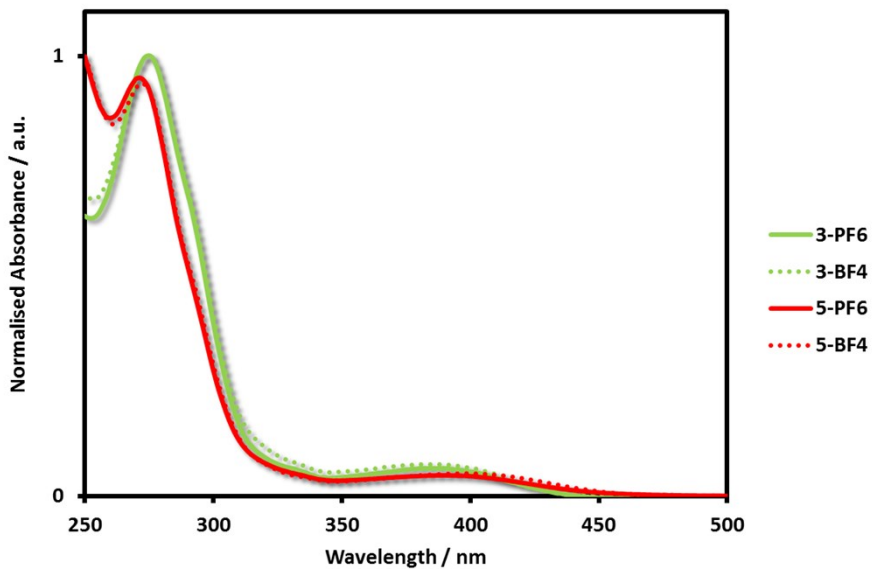


Figure S26: Cross comparison of UV in MeCN of complex **3**, **5**.

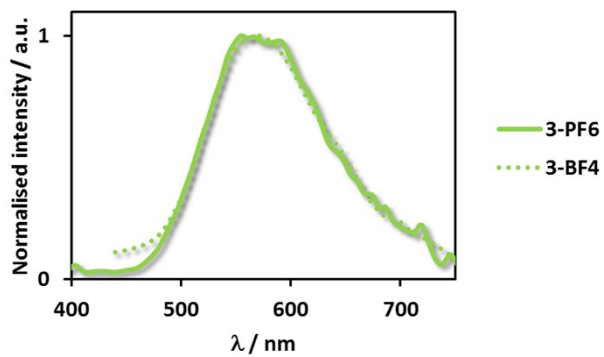


Figure S27: Cross comparison of PL in MeCN of complex **3** $\lambda_{\text{exc}} = 360$ nm.

11. NMR of the Synthesized of complexes

[Cu(dmphen)(p-CF₃-xantphos)]PF₆ ([1]PF₆)

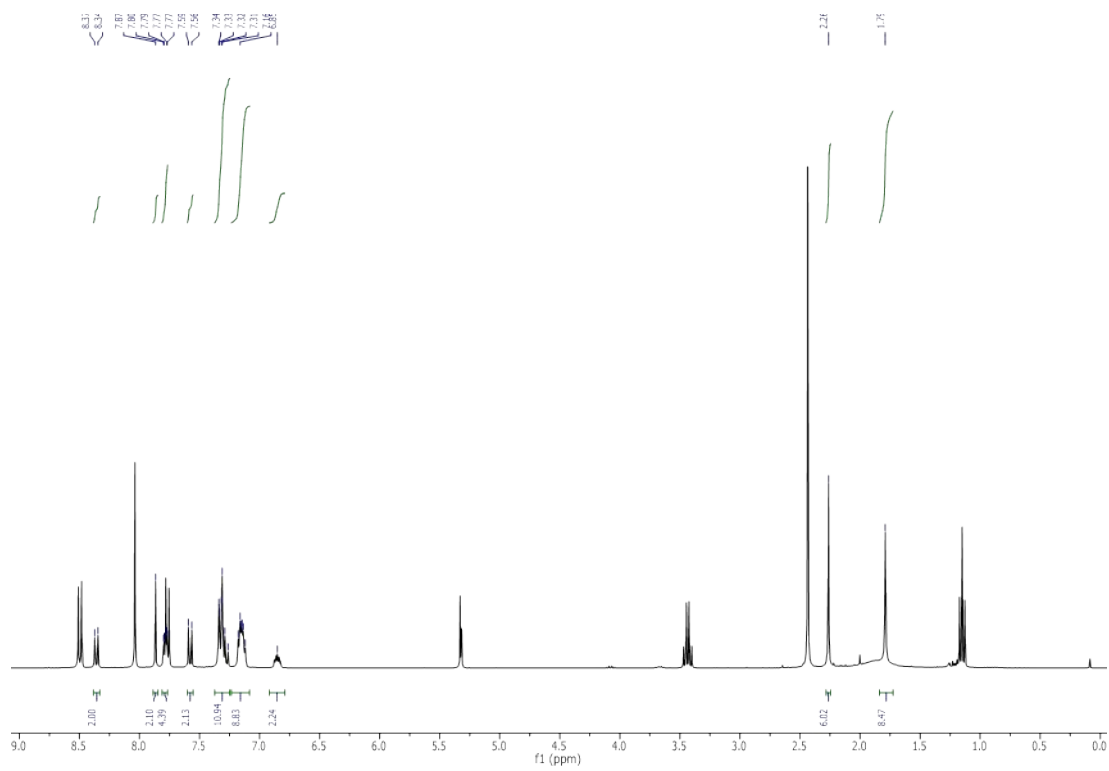


Figure S28: ¹H NMR (300 MHz, CD₂Cl₂, 298K) of 1

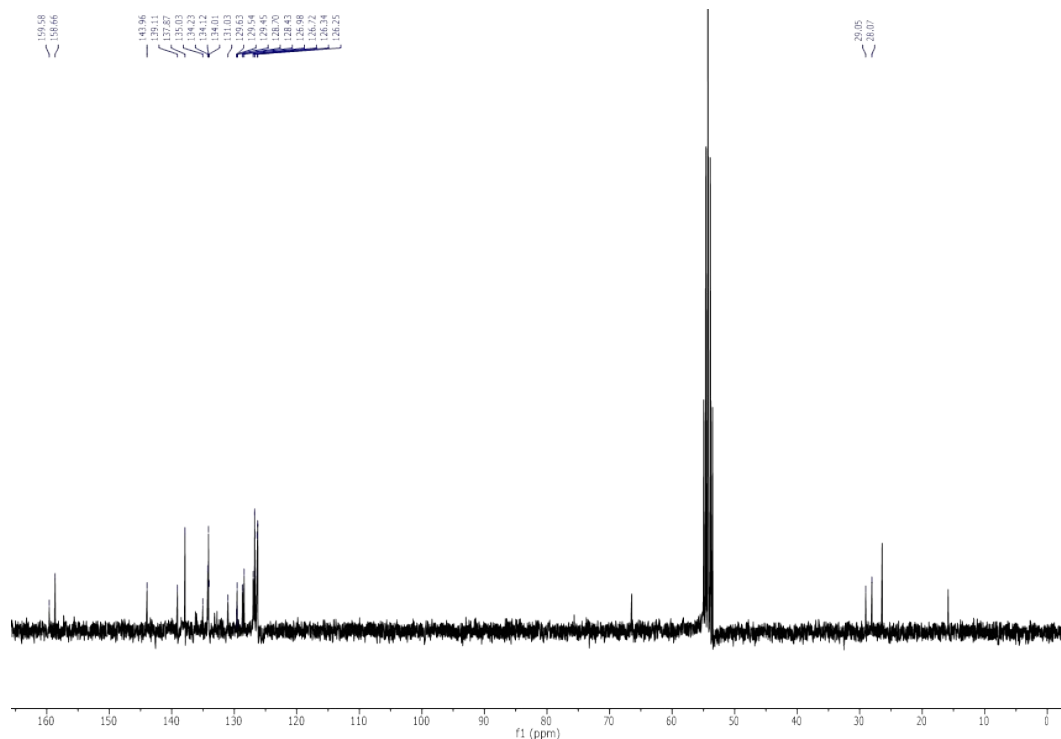


Figure S29: ^{13}C -{ ^1H } NMR (100 MHz, CD_2Cl_2 , 298K) of **1**

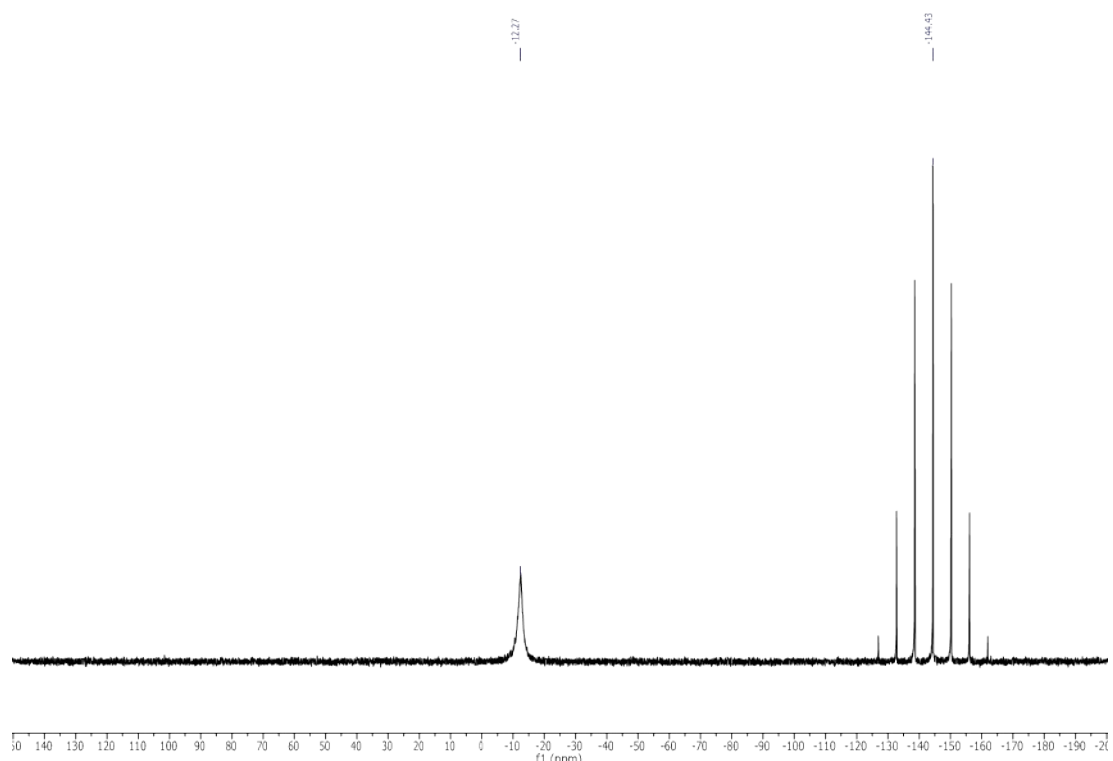


Figure S30: ^{31}P -{ ^1H } NMR (121 MHz, CD_2Cl_2 , 298K) of **1**

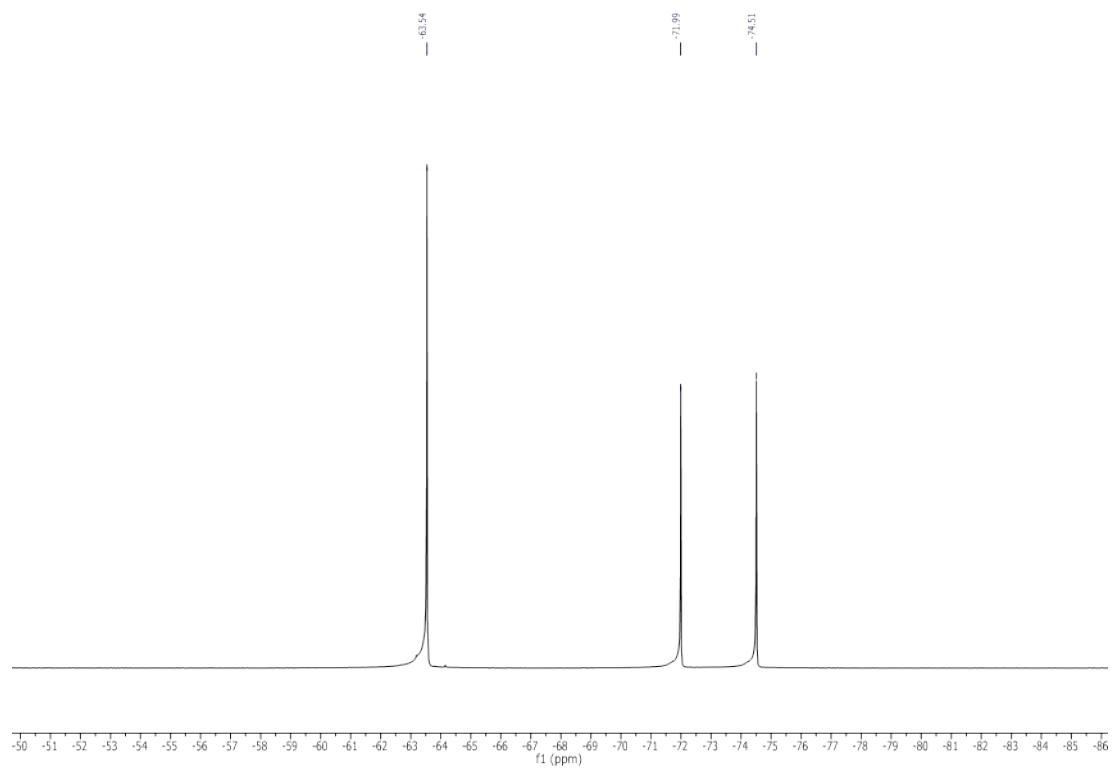


Figure S31: ^{19}F -{ ^1H } NMR (282 MHz, CD_2Cl_2 , 298K) of **1**

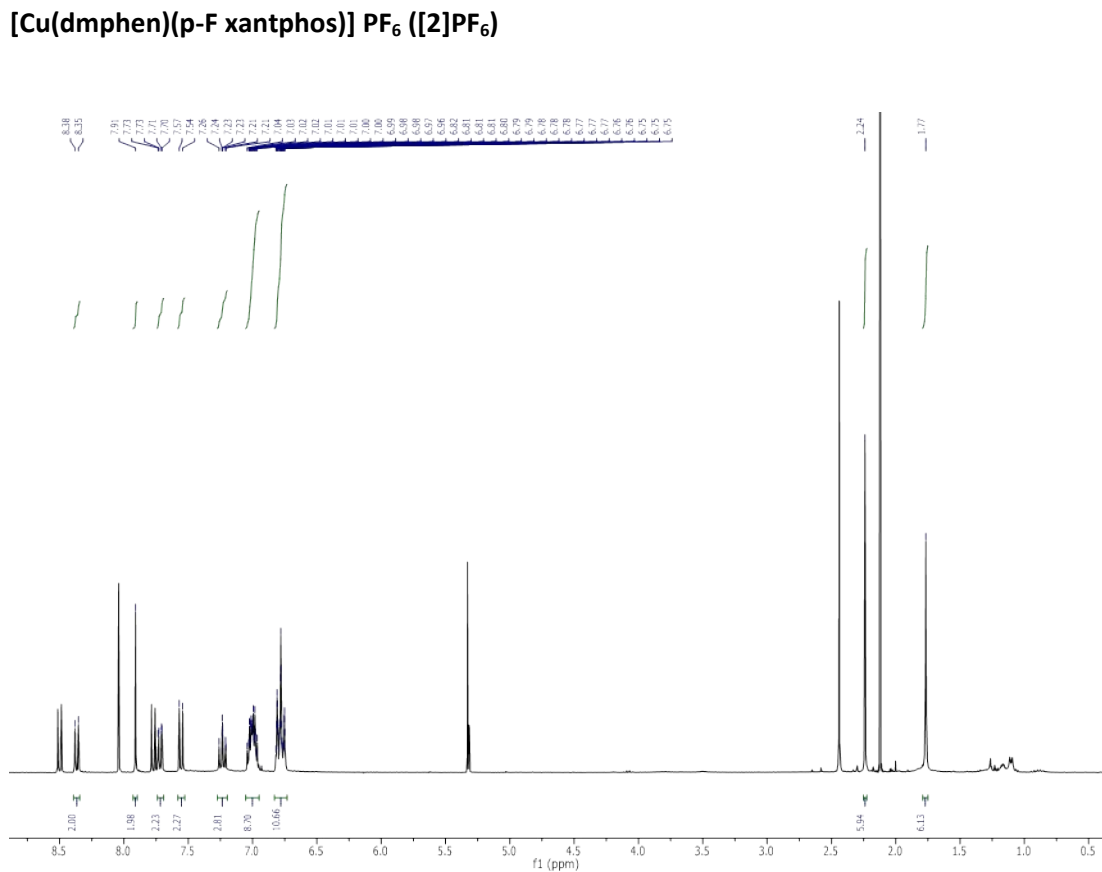


Figure S32: ^1H NMR (300 MHz, CD_2Cl_2 , 298K) of **2**

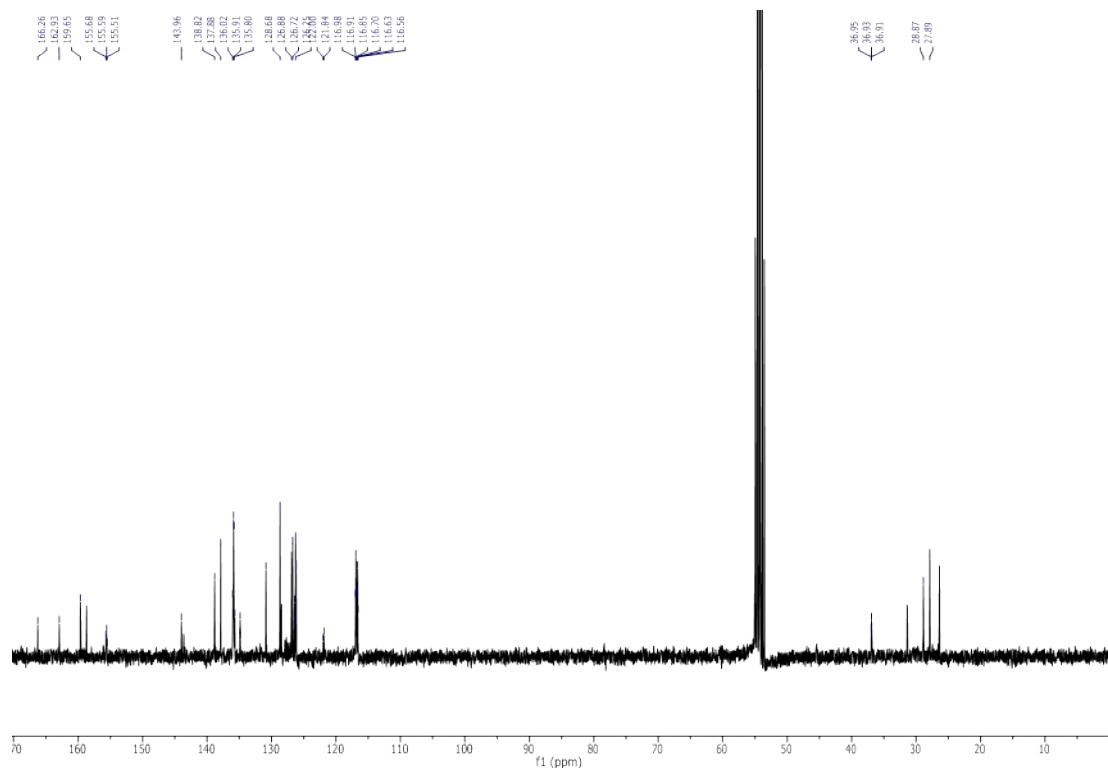


Figure S33: ^{13}C - $\{{}^1\text{H}\}$ NMR (100 MHz, CD_2Cl_2 , 298K) **2**

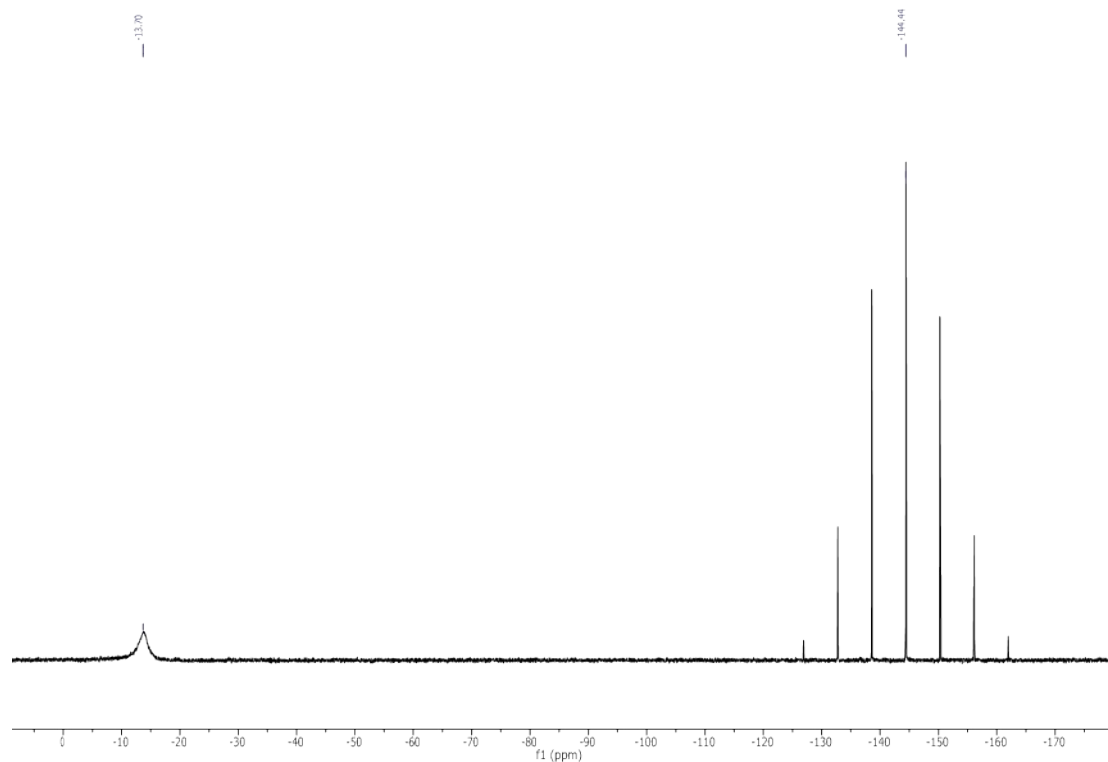


Figure S34: ^{31}P - $\{{}^1\text{H}\}$ NMR (121 MHz, CD_2Cl_2 , 298K) of **2**

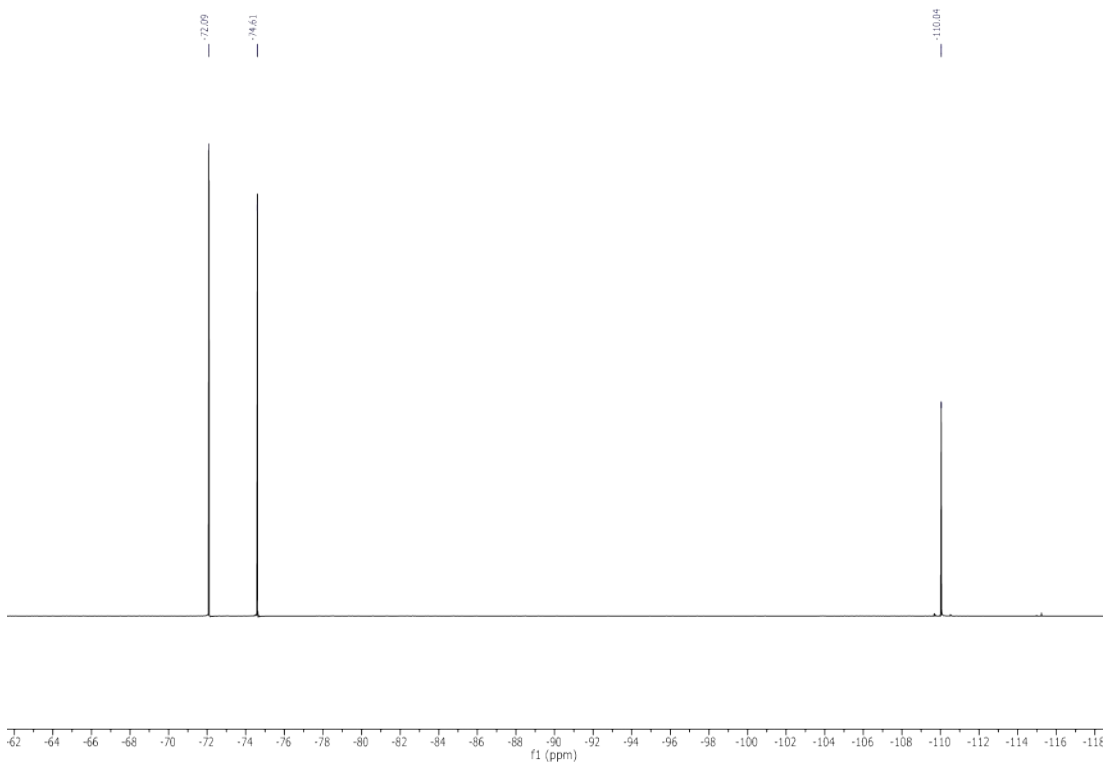


Figure S35: ^{19}F -{ ^1H } NMR (282 MHz, CD_2Cl_2 , 298K) of **2**

[Cu(dmphen)(p-H xantphos)] PF₆ ([3]PF₆)

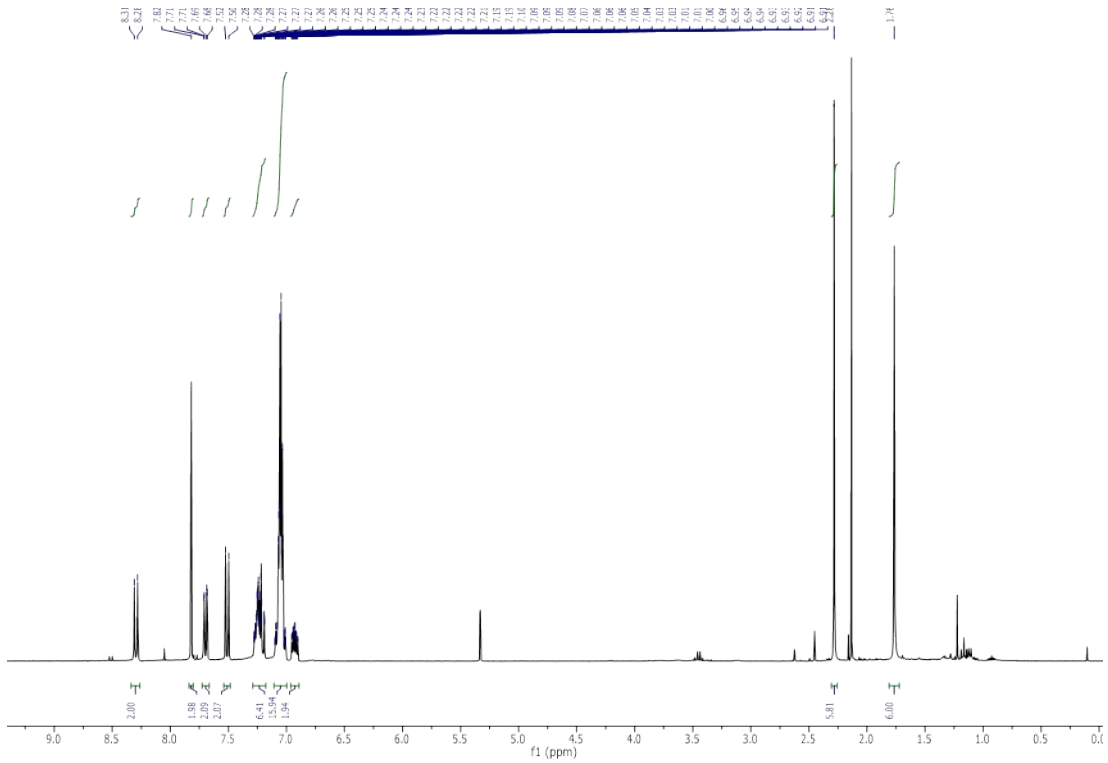


Figure S36: ^1H NMR (300 MHz, CD_2Cl_2 , 298K) of **3**

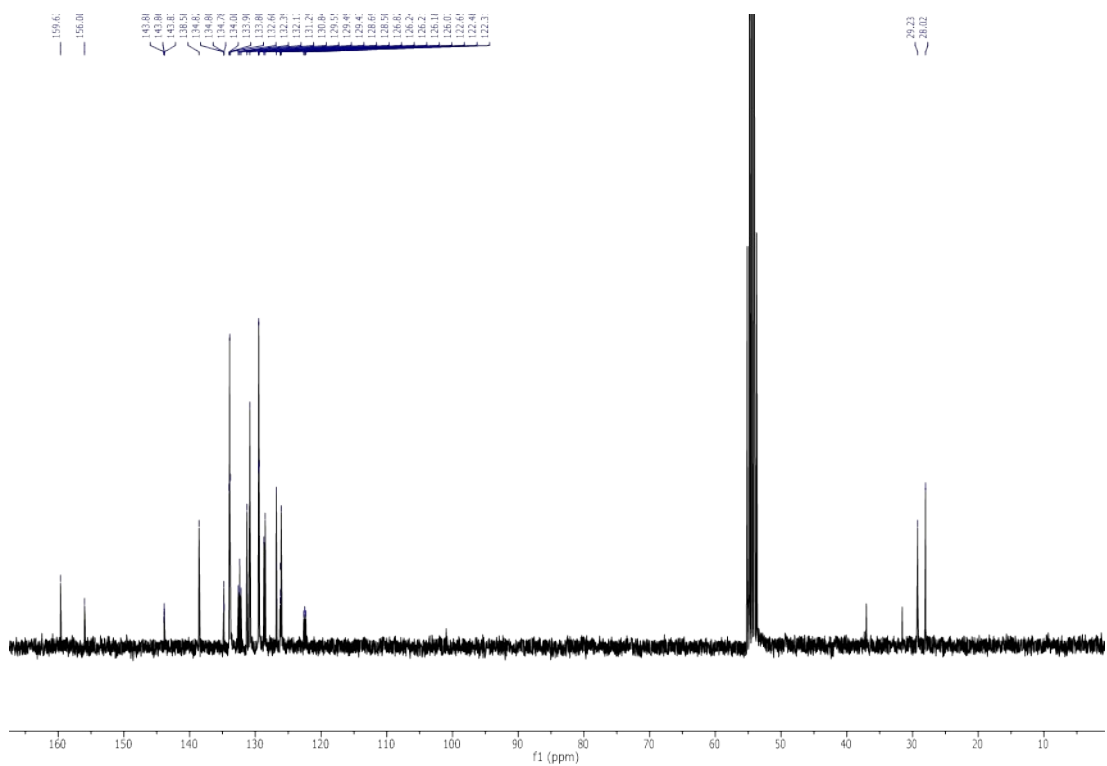


Figure S37: ^{13}C - $\{{}^1\text{H}\}$ NMR (100 MHz, CD_2Cl_2 , 298K) of **3**

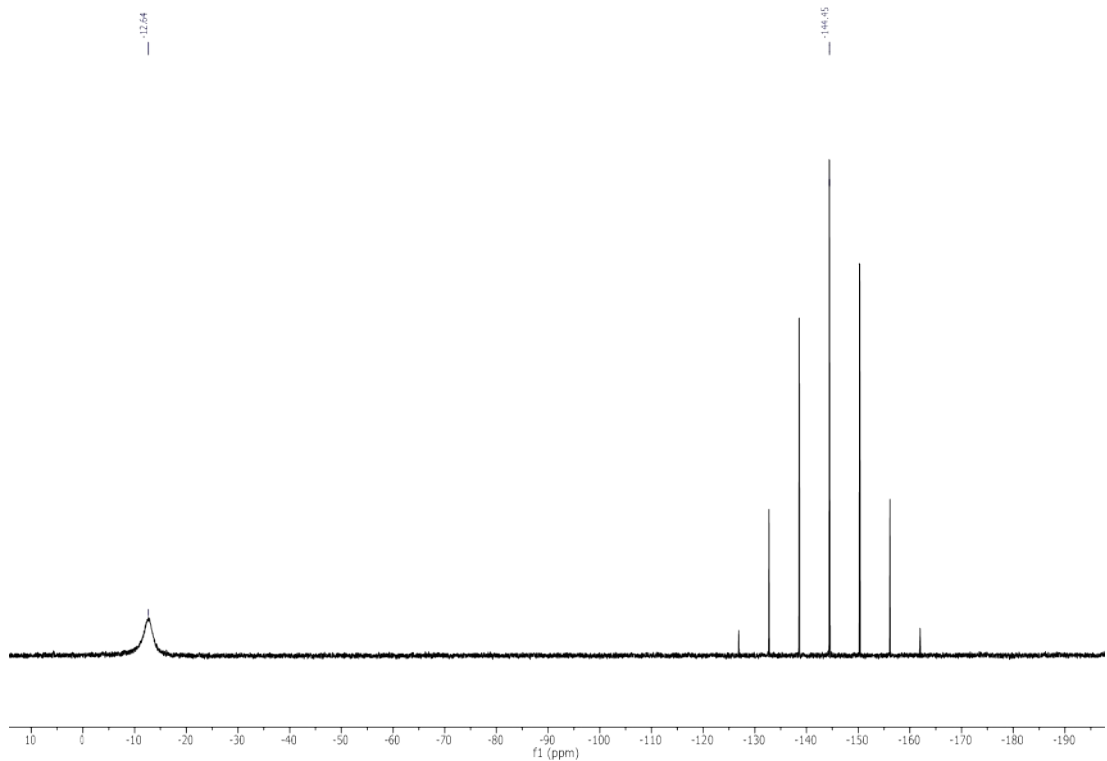


Figure S38: ^{31}P - $\{{}^1\text{H}\}$ NMR (121 MHz, CD_2Cl_2 , 298K) of **3**

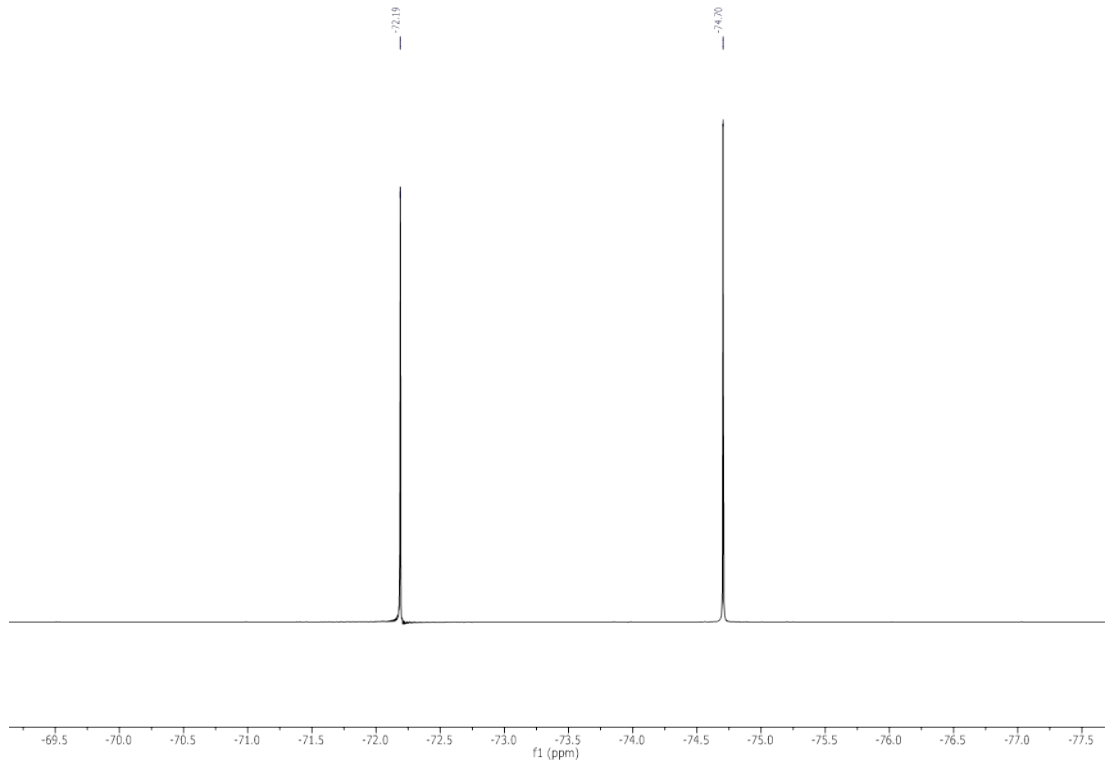


Figure S39: ^{19}F -{ ^1H } NMR (282 MHz, CD_2Cl_2 , 298K) of **3**

[Cu(dmpphen)(p-Me xantphos)] PF₆ ([4]PF₆)

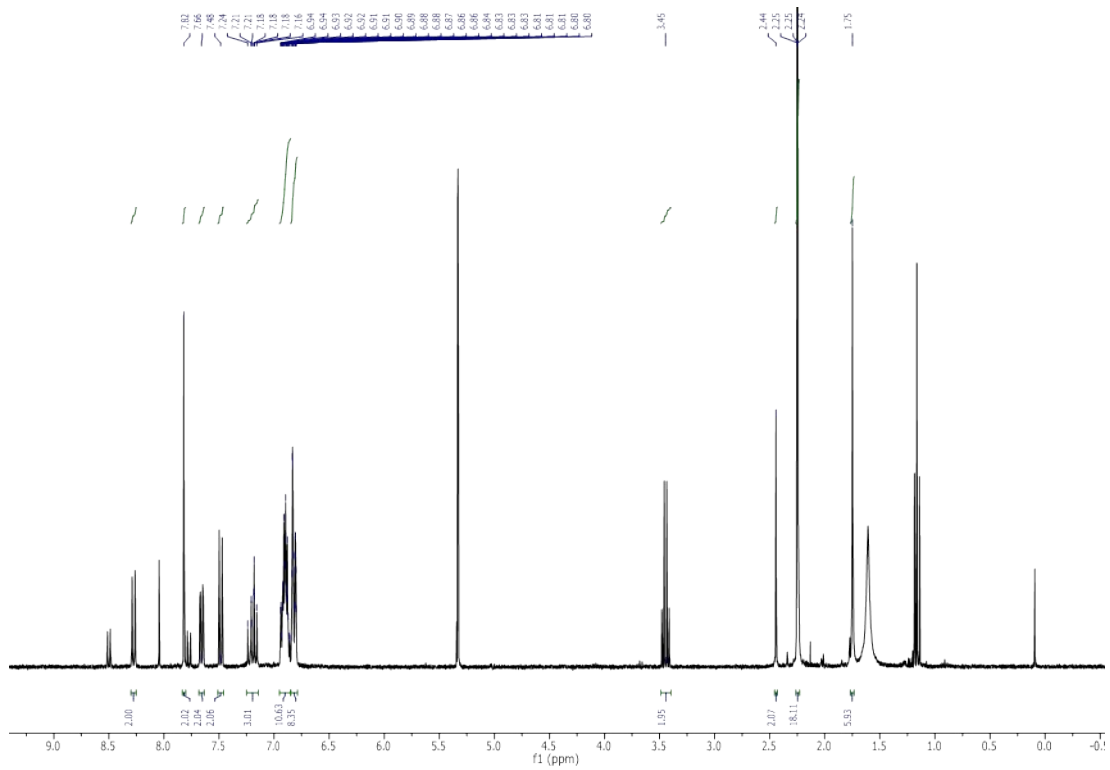


Figure S40: ^1H NMR (300 MHz, CD_2Cl_2 , 298K) of **4**

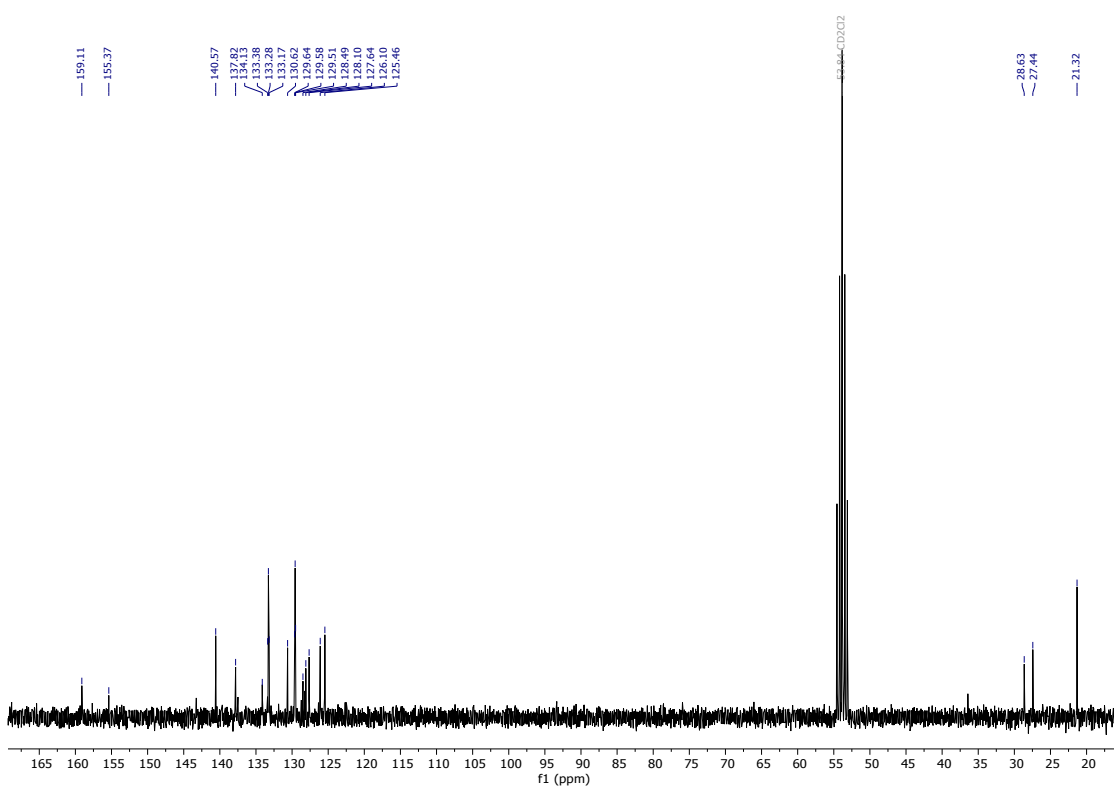


Figure S41: ¹³C-{¹H} NMR (100 MHz, CD₂Cl₂, 298K) of **4**

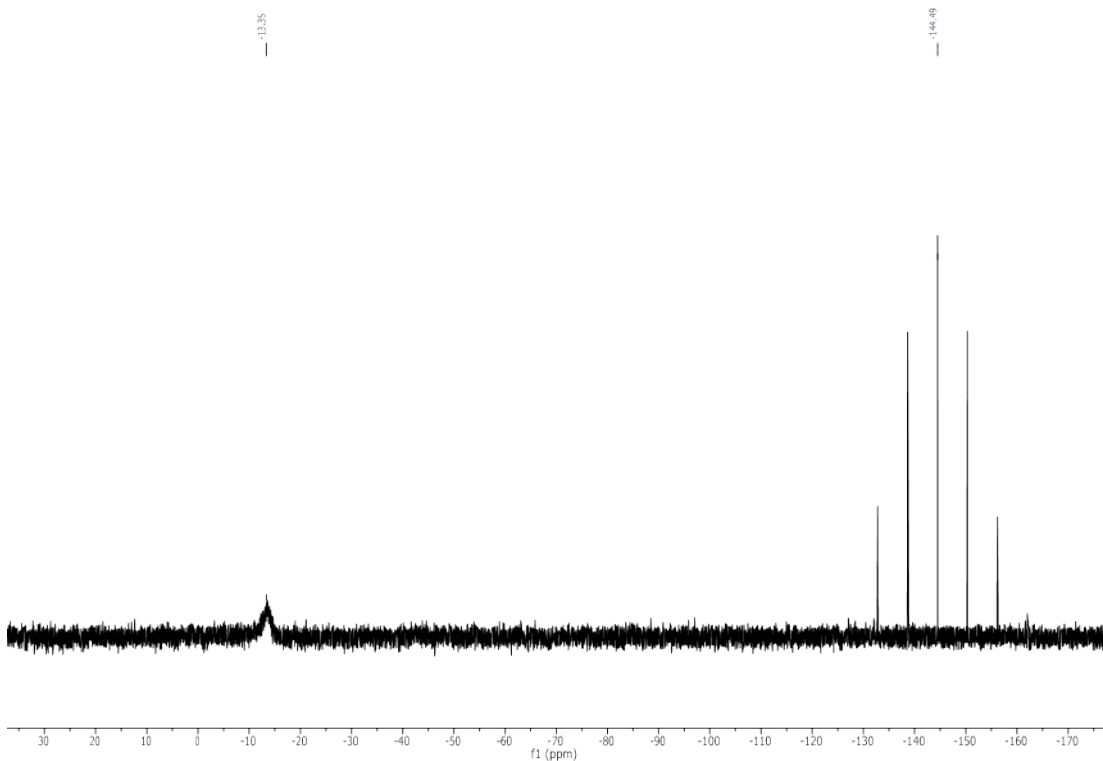


Figure S42: ³¹P-{¹H} NMR (121 MHz, CD₂Cl₂, 298K) of **4**

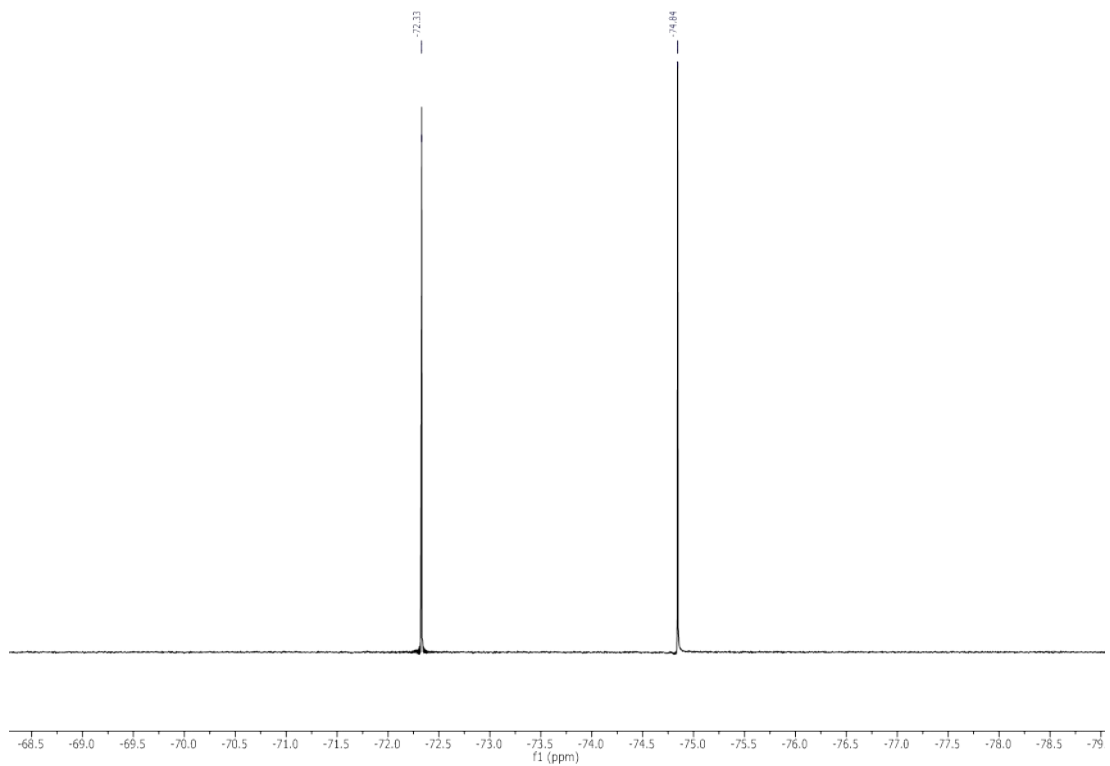


Figure S43: ^{19}F -{ ^1H } NMR (282 MHz, CD_2Cl_2 , 298K) of **4**

[Cu(dmphen)(p-OMe xantphos)] PF₆ ([5]PF₆)

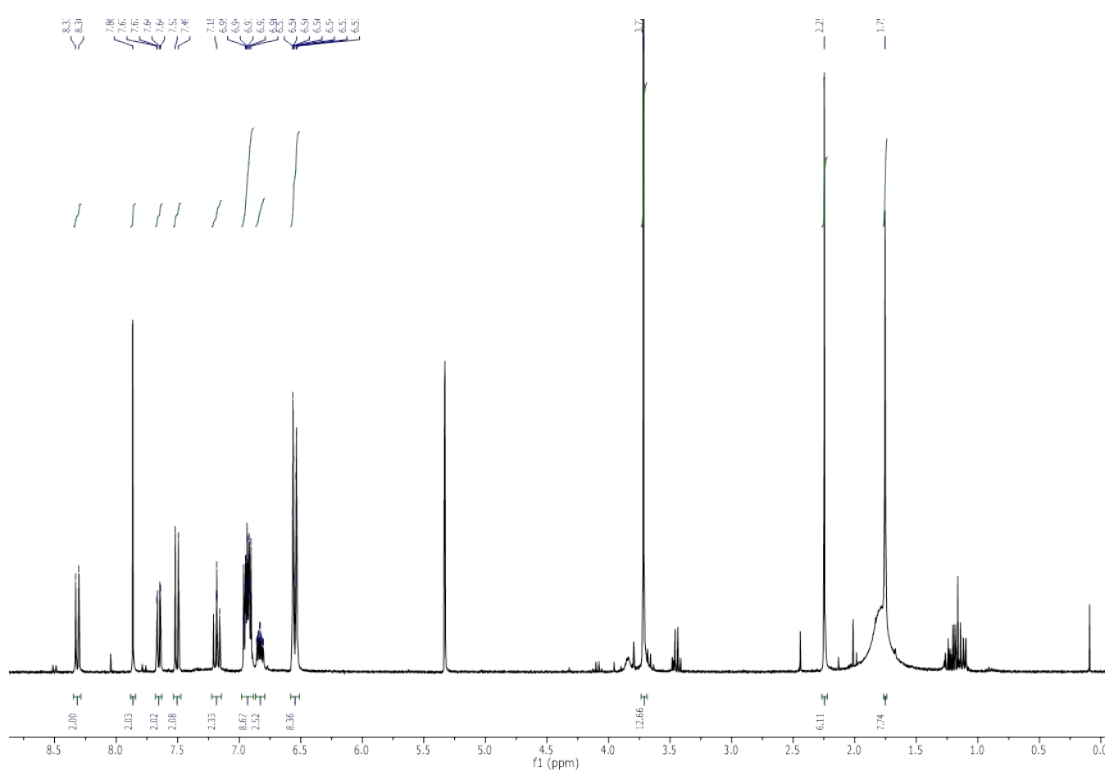
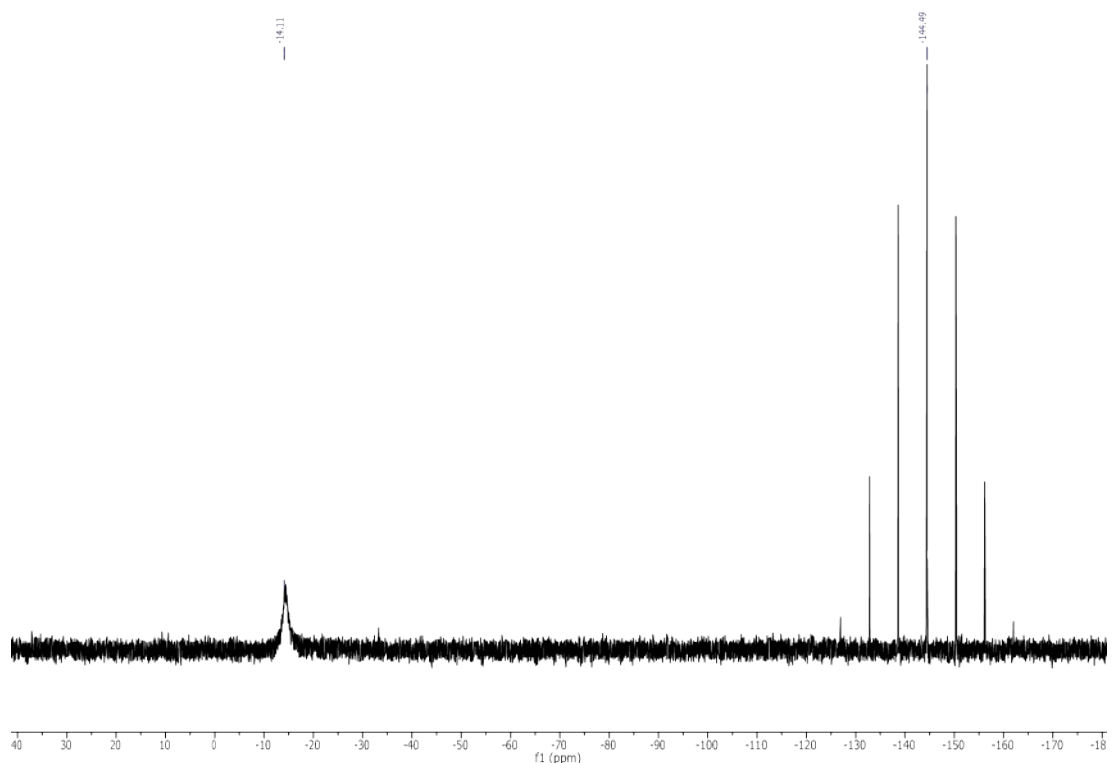
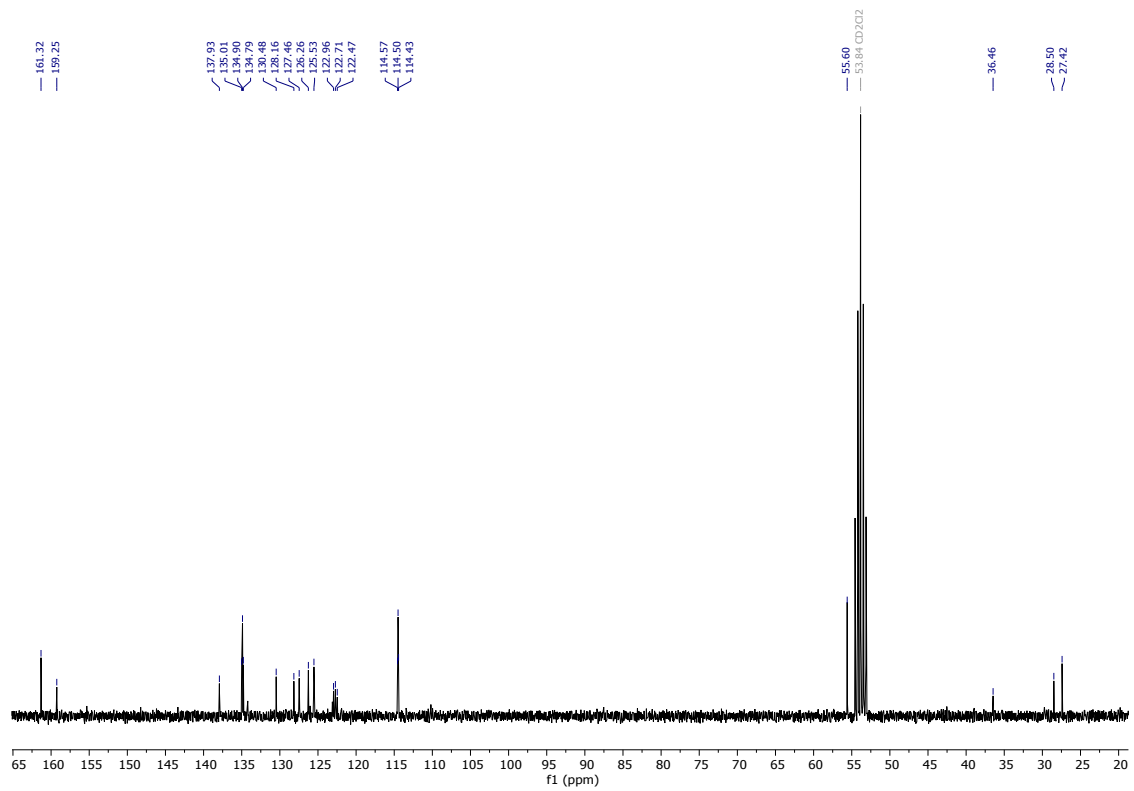


Figure S44: ^1H NMR (300 MHz, CD_2Cl_2 , 298K) of **5**



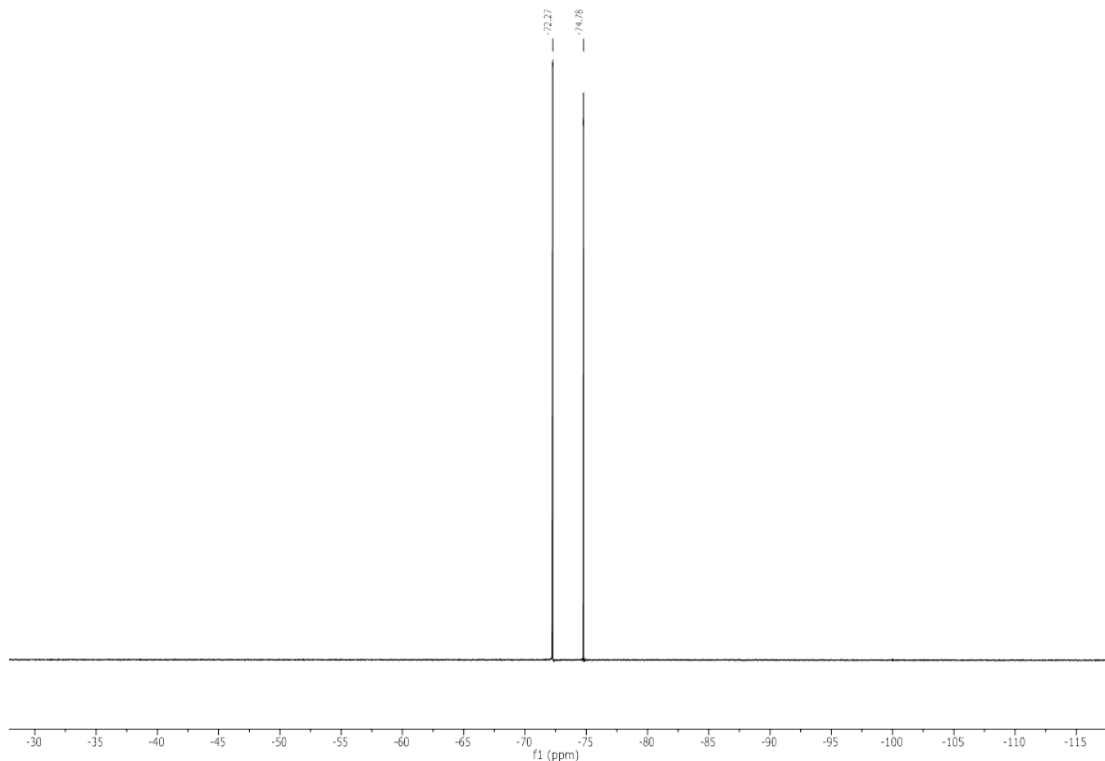


Figure S47: ¹⁹F-{¹H} NMR (282 MHz, CD₂Cl₂, 298K) of **5**

12. Optimized coordinates of complexes 1 - 5 (PBE0-D3/ECP1 optimized), xyz format

Complex 1

```

Cu -0.3658230 -0.8018930 0.0122180
P  1.8446690 -1.1581440 0.2323490
P  -1.2349150 1.1988190 0.7187280
F  5.5749990 2.7827550 -3.7984090
F  4.0408620 4.1175100 -3.0694330
F  5.8603760 3.8478220 -1.9322730
F  4.5666880 -6.4951770 -2.8524480
F  4.0948770 -7.3356270 -0.9195820
F  2.5824990 -7.2761090 -2.4641750
F  0.0034070 7.4156780 -1.5886200
F  1.5649830 6.3259460 -2.6244600
F  1.8605780 6.9601940 -0.5804500
F  -6.7650560 -0.2491840 -2.4967700
F  -7.6573640 1.4029350 -1.4353680
F  -7.5976010 -0.5598930 -0.5212990
O  1.0901980 0.7506450 2.3263960
N  -1.5892760 -1.0920200 -1.6988520
N  -1.7331820 -2.2311140 0.7659170
C  2.4172000 -2.7536360 -0.4394030
C  3.7583600 -3.0072710 -0.7544920
C  4.1349160 -4.2477230 -1.2512930
C  3.1741190 -5.2424820 -1.4348210
C  1.8386370 -4.9985450 -1.1308770
C  1.4609090 -3.7533150 -0.6391740
C  3.6045000 -6.5979830 -1.9264440

```

C -1.5228090 -0.4742220 -2.8736200
 C -0.3080040 0.3395520 -3.1766940
 C -2.5754630 -0.5554850 -3.8097040
 C -3.6997520 -1.2849440 -3.5139900
 C -3.7854050 -1.9525510 -2.2764770
 C -4.9220500 -2.7315100 -1.8991560
 C -4.9699810 -3.3453720 -0.6879050
 C -3.8934760 -3.2094120 0.2417370
 C -3.9193540 -3.7854660 1.5249380
 C -2.8687970 -3.5716190 2.3856410
 C -1.7781980 -2.7766480 1.9807570
 C -0.6425170 -2.5072310 2.9122360
 C -3.0065810 1.1658610 0.2958540
 C -3.4511220 1.7606200 -0.8925070
 C -4.7229870 1.4932990 -1.3790250
 C -5.5684310 0.6310470 -0.6830220
 C -5.1529820 0.0620290 0.5160070
 C -3.8747690 0.3200480 0.9973980
 C -6.9085450 0.3060530 -1.2739240
 C -1.1540090 1.4614090 2.5206530
 C -2.2061820 1.9097380 3.3236900
 C -2.0389760 2.0066190 4.7008250
 C -0.8210970 1.6733530 5.2905690
 C 0.2621410 1.2553740 4.5176090
 C 0.0626440 1.1636500 3.1413940
 C 1.6591620 0.9572000 5.0472550
 C 2.5401860 2.2013510 4.8001770
 C 1.6533760 0.6374970 6.5391280
 C 2.2175170 -0.1919200 4.2152730
 C 3.0423150 -1.2054680 4.7016350
 C 3.5661150 -2.1740720 3.8487850
 C 3.2666920 -2.1554430 2.4913900
 C 2.4257260 -1.1682420 1.9684060
 C 1.9250740 -0.2065500 2.8515570
 C 0.9524650 6.4812000 -1.4438220
 C 0.3764970 5.1823990 -0.9487950
 C 1.0273190 3.9886600 -1.2425570
 C 0.5237730 2.7916020 -0.7428470
 C -0.6259220 2.7845150 0.0486010
 C -1.2681740 3.9928650 0.3455200
 C -0.7709210 5.1879520 -0.1551410
 C 3.0725630 0.0127070 -1.9831740
 C 2.9271500 0.0660180 -0.5900830
 C 3.5101020 1.1214170 0.1159140
 C 4.1956750 2.1250220 -0.5597660
 C 4.3081730 2.0780960 -1.9459560
 C 4.9622900 3.2086080 -2.6880710
 C 3.7587590 1.0129720 -2.6583110
 C -2.6947960 -1.8136250 -1.3915410
 C -2.7577680 -2.4385510 -0.0961090
 H -1.2712550 6.1254070 0.0646460
 H -2.1594000 3.9990820 0.9672330
 H 1.9195300 3.9943840 -1.8593530
 H 1.0337170 1.8598200 -0.9606140
 H -2.7949280 2.4251490 -1.4468780
 H -3.5448390 -0.1617860 1.9138430
 H -5.8158550 -0.6037110 1.0574710
 H -5.0557430 1.9452220 -2.3087230

H 4.6448660 2.9441960 -0.0078420
 H 3.4285610 1.1704700 1.1963630
 H 2.6583920 -0.8218100 -2.5429640
 H 3.8748470 0.9653400 -3.7364170
 H 4.5059000 -2.2303150 -0.6197630
 H 5.1718920 -4.4440510 -1.5051250
 H 1.0970460 -5.7735290 -1.2932980
 H 0.4160750 -3.5468480 -0.4186760
 H 3.6665700 -2.9251200 1.8394780
 H 4.2125660 -2.9501120 4.2465090
 H 3.2874660 -1.2413340 5.7577970
 H 1.2680200 1.4853230 7.1126250
 H 1.0429610 -0.2430360 6.7653260
 H 2.6708040 0.4592060 6.8989570
 H 2.5595940 2.4713450 3.7395600
 H 2.1502050 3.0566880 5.3618480
 H 3.5674160 2.0066350 5.1262100
 H -0.7157940 1.7541800 6.3673330
 H -2.8619620 2.3468000 5.3217110
 H -3.1609180 2.1619240 2.8718560
 H -0.5230670 1.4103000 -3.0731670
 H 0.4968510 0.0924150 -2.4825770
 H 0.0366410 0.1720670 -4.2022380
 H -2.4814060 -0.0342730 -4.7572650
 H -4.5246350 -1.3526450 -4.2175620
 H -5.7512780 -2.8099950 -2.5948880
 H -5.8343770 -3.9365010 -0.3991210
 H -4.7717380 -4.3889720 1.8256790
 H -2.8678350 -4.0034750 3.3809540
 H -0.5903020 -1.4394620 3.1511210
 H -0.7536650 -3.0609380 3.8474300
 H 0.3122980 -2.7848180 2.4555250

Complex 2

Cu -0.6940230 -0.4926200 0.0150910
 P -0.5271530 1.7740320 -0.2292020
 P 1.3242000 -1.5454750 -0.0275730
 F 0.7952340 -7.4370680 -0.2862990
 F 4.6163390 0.0552990 -4.7063810
 F 3.2537570 3.4710510 -4.4718180
 F -5.6262520 4.5703670 -1.3494590
 O 1.8437460 1.0351090 1.1988200
 N -2.2674530 -1.3421760 -1.1525860
 N -2.1026600 -0.9932750 1.5367920
 C -3.2927280 -1.3800030 1.0143400
 C -2.0894500 3.8726940 -1.3209320
 C 0.0699870 2.5724260 1.3005240
 C 2.4158950 0.0520210 1.9697790
 C 1.2270810 2.0524100 1.8829350
 C 0.6420650 2.3633890 -1.5023880
 C 2.4247110 -1.1009920 -1.4233300
 C 2.3270120 -1.2530550 1.4801420
 C 1.7024030 3.2304710 -1.2245930
 C -3.3821430 -1.5603250 -0.4114670
 C -0.5969050 3.5953440 1.9779210
 C 2.3076580 -1.7875630 -2.6390120
 C 1.7441490 2.4888080 3.0997090

C 3.0018720 0.3857190 3.1892110
 C 3.4696420 -1.9746620 3.4856170
 C -4.4367630 -1.6142080 1.8105880
 C 3.3125090 -0.0218880 -1.3441930
 C 2.3090920 -4.1723660 -0.4519140
 C 3.5246930 -0.6614620 3.9473480
 C -0.0276370 -3.9539850 0.1220780
 C 2.3966980 3.1240520 -3.5115010
 C -3.2921510 4.5202050 -1.5756820
 C 1.3391980 2.2797430 -3.8253500
 C 1.2119470 -3.3579840 -0.1354620
 C 1.0389980 3.4964180 3.7598710
 C -4.2973580 -1.4432510 3.2013050
 C 2.8770000 -2.2726710 2.2629410
 C 0.9292980 -6.1128700 -0.2352760
 C -2.3115400 -1.5481180 -2.4640010
 C 0.4689270 1.9025280 -2.8132330
 C -0.1150640 4.0459600 3.2039250
 C -3.0802730 -1.0718060 3.7171450
 C -1.0565590 -1.3860800 -3.2569490
 C 2.1738050 -5.5529210 -0.5033220
 C -4.6099010 -1.9653740 -0.9792760
 C -0.1770740 -5.3356500 0.0767340
 C 3.0464940 -1.4052790 -3.7523190
 C -5.7504240 -2.1775780 -0.1458570
 C 3.0514290 1.8618240 3.5708620
 C 3.9103730 -0.3254940 -3.6407990
 C 4.0611560 0.3658130 -2.4477140
 C 3.2775750 2.0618120 5.0661930
 C -4.4811840 2.7652470 -0.3867410
 C -3.2722350 2.1252910 -0.1454890
 C -4.4700640 3.9547060 -1.1035760
 C 2.5862580 3.6140770 -2.2279350
 C -5.6664020 -2.0093910 1.2003270
 C -0.6637250 -0.4258510 3.4014830
 C 4.2079670 2.5241720 2.7913580
 C -3.5018130 -1.9478810 -3.1095100
 C -4.6438180 -2.1477930 -2.3763000
 C -1.9862090 -0.8482800 2.8551870
 C -2.0672350 2.6699630 -0.6051430
 H -2.9443400 -0.9433170 4.7858720
 H -0.8825590 -3.3243150 0.3552180
 H 3.2740730 -3.7216740 -0.6679410
 H 3.0098080 -6.1999220 -0.7475170
 H -1.1302840 -5.8152300 0.2729510
 H -5.1508660 -1.6139810 3.8519840
 H -6.5311010 -2.1765740 1.8362310
 H -6.6839880 -2.4816920 -0.6105540
 H -5.5700330 -2.4523570 -2.8561120
 H -3.4957870 -2.0951880 -4.1849560
 H -0.7034190 -2.3656860 -3.6015920
 H -1.2254120 -0.7745280 -4.1500550
 H -0.2673000 -0.9338990 -2.6545400
 H 0.1446110 -1.0064430 2.9488740
 H -0.4802700 0.6296720 3.1729080
 H -0.6217520 -0.5500520 4.4862810
 H 2.8151050 -3.3029620 1.9286200
 H 3.8880790 -2.7744900 4.0887310

H 3.9825560 -0.4566620 4.9094160
 H 5.1632450 2.0687750 3.0730320
 H 4.0774920 2.4063030 1.7107290
 H 4.2501020 3.5952260 3.0166270
 H 3.3277130 3.1274620 5.3079810
 H 2.4804630 1.6058770 5.6628710
 H 4.2339030 1.6283430 5.3727400
 H 1.3927280 3.8649230 4.7172660
 H -0.6412260 4.8356840 3.7312760
 H -1.4994080 4.0223710 1.5516440
 H -3.3317200 5.4507260 -2.1322120
 H -5.4241510 2.3568350 -0.0386000
 H -1.1612550 4.3024430 -1.6865950
 H -3.2604760 1.1923500 0.4100610
 H 1.2208410 1.9252150 -4.8437060
 H 3.4153690 4.2850240 -2.0281960
 H -0.3649320 1.2486630 -3.0480390
 H 1.8441780 3.6152480 -0.2192440
 H 4.7518820 1.2004570 -2.3972300
 H 2.9684220 -1.9359740 -4.6954820
 H 1.6443850 -2.6436530 -2.7179780
 H 3.4219870 0.5332050 -0.4207160

Complex 3

Cu -0.7900790 -0.1928040 0.0002720
 P 0.1192240 1.7858430 0.6780110
 P 0.6414870 -1.9594710 0.1658670
 O 2.3410020 0.3419210 -0.4186500
 N -2.7799910 -0.5214560 0.6780870
 N -1.8865440 0.0706190 -1.8185280
 C -4.5659530 -0.9024280 2.2222440
 C -5.5078480 -0.6350840 1.2619550
 C -5.0906810 -0.3128560 -0.0452310
 C -6.0106660 -0.0350820 -1.1015660
 C -5.5638150 0.2635760 -2.3502920
 C -3.7000450 -0.2716300 -0.2867810
 C -3.2266320 0.0421250 -1.6095380
 C -4.1646610 0.3062560 -2.6325780
 C -3.6543560 0.6035160 -3.9118460
 C -2.2965450 0.6193680 -4.1094300
 C -1.4231070 0.3483980 -3.0340950
 C 0.0542400 0.3919010 -3.2366680
 C -2.1721530 -1.1698480 2.9381570
 C -1.0410000 3.1712630 0.9225600
 C -2.2194610 3.1779150 0.1682650
 C -3.1301260 4.2216490 0.2965220
 C -2.8738850 5.2610250 1.1877890
 C -1.7041230 5.2581300 1.9451680
 C -0.7876150 4.2192410 1.8137330
 C 1.0992070 1.7611410 2.2213340
 C 0.4685960 1.3136600 3.3877270
 C 1.1639650 1.2558070 4.5887310
 C 2.5016760 1.6426290 4.6383400
 C 3.1337210 2.0961070 3.4846300
 C 2.4369320 2.1589230 2.2804240
 C 0.7819360 -2.8991980 2.8004510
 C 1.3120910 -2.9779180 4.0841500

C 2.4975240 -2.3165470 4.3923920
 C 3.1505270 -1.5794670 3.4089230
 C 2.6232150 -1.4956080 2.1248400
 C 1.4325860 -2.1566850 1.8070330
 C 2.0289960 -1.9131770 -1.0355070
 C 2.3610910 -2.9788800 -1.8775830
 C 3.3074110 -2.8105380 -2.8826280
 C 3.6395840 -0.4963090 -2.2443110
 C 4.2867640 0.8819650 -2.3340330
 C 3.2006110 1.9033070 -2.0156480
 C 2.2938670 1.5787750 -1.0106630
 C 1.2895170 2.4378300 -0.5636120
 C 1.1934340 3.6945190 -1.1650990
 C 2.0685960 4.0428190 -2.1905500
 C 3.0593120 3.1570640 -2.6120670
 C 5.3712570 0.9802920 -1.2395990
 C 4.9257590 1.1294460 -3.6967190
 C 3.9330590 -1.5802720 -3.0705610
 C 2.6948840 -0.7020850 -1.2398830
 C -0.1392710 -3.5770310 -0.1432650
 C -1.3818650 -3.5881990 -0.7847380
 C -2.0178670 -4.7947720 -1.0653950
 C -1.4180810 -5.9971480 -0.7026470
 C -0.1800290 -5.9948610 -0.0604070
 C 0.4585920 -4.7917610 0.2188370
 C -3.1926350 -0.8429280 1.8985960
 H 4.1915450 1.0682250 -4.5069990
 H 5.3965990 2.1164560 -3.7272820
 H 5.7183910 0.4005640 -3.8890310
 H 5.8323100 1.9737470 -1.2531920
 H 4.9464590 0.8129670 -0.2446000
 H 6.1500770 0.2294550 -1.4103020
 H 3.7318260 3.4542710 -3.4100360
 H 1.9840270 5.0171220 -2.6621050
 H 0.4240870 4.3883040 -0.8407130
 H 4.6567100 -1.4702340 -3.8715180
 H 3.5537690 -3.6440940 -3.5331680
 H 1.8565850 -3.9324620 -1.7636890
 H 2.9364230 2.5277120 1.3896780
 H -0.5766930 1.0222480 3.3558590
 H 0.6636270 0.9042040 5.4863050
 H 3.0477260 1.5945070 5.5760640
 H 4.1730090 2.4109210 3.5200170
 H 3.1385530 -0.9045420 1.3773780
 H -0.1340350 -3.4336460 2.5658320
 H 0.8010140 -3.5661210 4.8413020
 H 2.9135900 -2.3803010 5.3936830
 H 4.0747010 -1.0589460 3.6405370
 H 0.1230750 4.2177730 2.4061790
 H -1.5041700 6.0683920 2.6404190
 H -3.5870180 6.0733530 1.2948720
 H -4.0424420 4.2196120 -0.2933750
 H -2.4172720 2.3622270 -0.5212820
 H 0.3244860 0.0991680 -4.2552370
 H 0.4321300 1.4076340 -3.0681660
 H 0.5548420 -0.2745020 -2.5325820
 H -2.2658360 -2.2182560 3.2446460
 H -1.1610910 -1.0143830 2.5584680

H -2.3166220 -0.5602270 3.8373550
 H 1.4194080 -4.7916710 0.7270490
 H 0.2876190 -6.9330930 0.2239150
 H -1.9151000 -6.9388960 -0.9170700
 H -2.9832580 -4.7949710 -1.5634800
 H -1.8463540 -2.6449670 -1.0609980
 H -1.8771770 0.8393500 -5.0858970
 H -4.3403850 0.8114290 -4.7286870
 H -6.2625810 0.4729640 -3.1552820
 H -7.0747840 -0.0693760 -0.8857630
 H -6.5689880 -0.6732120 1.4932220
 H -4.8585900 -1.1624990 3.2347390

Complex 4

Cu -0.3557920 0.6613420 0.1208570
 P -0.9144100 -1.5476930 -0.0557750
 P 1.8089500 1.2595850 0.2432640
 O 1.7002950 -1.2903060 -1.2244790
 N -1.6366200 1.5893700 -1.2919250
 N -1.9483890 1.2849670 1.3872270
 C -2.8395540 1.8944670 -0.7512860
 C -3.0127360 1.7101440 0.6662170
 C -2.0896350 1.0705500 2.6911250
 C 1.0398710 3.9146400 0.1356620
 C 2.0866390 3.0446630 0.4530330
 C -1.4563290 1.7210090 -2.6050880
 C 4.2015540 -1.2400330 2.4774360
 C 3.6079770 1.7244730 -1.9153180
 C -4.2756130 1.9606610 1.2444120
 C 4.0397230 -0.7646430 3.7808290
 C -3.3217150 1.2884500 3.3431100
 C 3.9819810 0.1253960 -3.6874870
 C -0.3625440 -2.7286470 1.2156500
 C 2.7563750 0.8262890 -1.2652160
 C -4.4060290 1.7311530 2.6275210
 C 3.1545200 -0.8052380 -3.0606000
 C -0.3814290 -2.3384560 -1.6131010
 C 4.2096220 1.3765980 -3.1195030
 C 3.4554680 4.9535120 1.0280000
 C -3.9300880 2.3516580 -1.5254100
 C 3.2994620 3.5798120 0.9074500
 C 2.4135570 5.8323530 0.7041340
 C 0.6050250 -2.3323120 2.1382360
 C 3.2439700 0.3704850 3.9706250
 C 3.5866150 -0.6153280 1.3976650
 C 2.8992800 -2.2248270 -3.5548150
 C 2.7820350 0.5091110 1.5959370
 C 2.6255720 1.0008840 2.8986040
 C -5.1880490 2.6186510 -0.9022690
 C -3.7194330 2.4939550 -2.9087340
 C -0.8458490 -4.0437880 1.2593380
 C -5.3559020 2.4243980 0.4323170
 C 1.2072040 5.2907510 0.2555020
 C -2.7316150 -1.6532980 -0.0528700
 C -1.1790910 -3.1565610 -2.4175090
 C -2.4918550 2.1803190 -3.4430830
 C -0.1242200 1.3485310 -3.1672240

C -3.4216140 -1.9307830 1.1309040
 C 0.9222080 -2.0742550 -2.0425570
 C 4.7232070 -1.4312240 4.9398670
 C 0.6059110 -3.3336820 -4.0376900
 C 0.5922420 -4.5354760 3.1534080
 C 3.2241430 -2.3855900 -5.0366920
 C -0.9113540 0.5651700 3.4560330
 C 1.0758450 -3.2287840 3.0944240
 C -3.4640280 -1.2047500 -1.1621420
 C 1.4437110 -2.5499590 -3.2447780
 C 3.7888470 -3.1854890 -2.7359790
 C -4.8413530 -1.0543200 -1.0857210
 C -0.3767810 -4.9280290 2.2186410
 C -0.6881460 -3.6436380 -3.6241560
 C 2.5532610 -0.4216130 -1.8616380
 C -5.5350240 -1.3186320 0.1003910
 C -4.8013290 -1.7620110 1.2014690
 C -7.0196960 -1.1127530 0.1777720
 C 1.0915520 -5.5053230 4.1849130
 C 2.5892680 7.3145690 0.8629280
 H 4.9253010 -2.4866050 4.7327040
 H 5.6859010 -0.9507130 5.1546040
 H 4.1202800 -1.3693950 5.8514810
 H 3.1112220 0.7689920 4.9737700
 H 2.0276650 1.8920180 3.0743060
 H 4.8188950 -2.1177500 2.3021350
 H 3.7317180 -1.0159370 0.3998520
 H 4.1185540 2.9162930 1.1727810
 H 0.0886160 3.5062470 -0.1998850
 H 0.3844310 5.9556870 0.0043040
 H 4.4018790 5.3561160 1.3814400
 H 1.7972650 7.8700400 0.3528760
 H 2.5656210 7.5987130 1.9221860
 H 3.5525040 7.6464890 0.4614310
 H 1.4964200 -6.4088160 3.7149220
 H 1.8790250 -5.0632000 4.8016950
 H 0.2817280 -5.8250470 4.8512410
 H -0.7613230 -5.9450620 2.2439040
 H 1.8359020 -2.9013390 3.7991350
 H 1.0053940 -1.3248980 2.1022270
 H -1.5924400 -4.3725370 0.5406740
 H -2.8788350 -2.2793280 2.0051400
 H -2.9526720 -0.9611680 -2.0902070
 H -5.3881350 -0.7072090 -1.9594070
 H -5.3170840 -1.9797590 2.1336790
 H -7.5475750 -1.7346670 -0.5542100
 H -7.4087830 -1.3600000 1.1695740
 H -7.2796420 -0.0693420 -0.0379670
 H 2.6179660 -1.7209840 -5.6612880
 H 4.2806210 -2.1728620 -5.2241830
 H 3.0539420 -3.4171970 -5.3583590
 H 0.9658590 -3.7196910 -4.9857540
 H -1.3168800 -4.2706190 -4.2490770
 H -2.1927780 -3.3905220 -2.1064470
 H 4.4610470 -0.1257200 -4.6279460
 H 4.8619020 2.0853710 -3.6203680
 H 3.7777470 2.7071960 -1.4874860
 H 4.8462750 -2.9511260 -2.8989020

H 3.5778540 -3.1057690 -1.6649400
 H 3.6067310 -4.2209060 -3.0429280
 H 0.0110320 0.7539840 2.9045730
 H -0.8454190 1.0362900 4.4418880
 H -0.9879660 -0.5183070 3.6102170
 H -3.3945480 1.1041480 4.4103620
 H -5.3616940 1.9086700 3.1136450
 H -6.3140790 2.6192550 0.9061310
 H -6.0086670 2.9723230 -1.5202940
 H -4.5297770 2.8444100 -3.5426820
 H -2.3064410 2.2783310 -4.5076510
 H -0.0590030 1.5849240 -4.2319800
 H 0.6803250 1.8721960 -2.6422760
 H 0.0528920 0.2743480 -3.0432280

Complex 5

Cu -0.2173950 -0.8237160 0.0779120
 P -1.8217110 0.7824500 -0.0549270
 P 1.9306620 -0.1115940 -0.2215050
 O 0.3534590 1.6519800 -1.8398850
 O 5.5280480 -4.6702760 1.1496580
 O 4.2216250 4.8463030 2.2246680
 O -0.6682210 5.4938910 3.4354430
 O -7.2565630 -1.2245490 1.3567160
 N -0.2881160 -2.2876450 1.6037600
 N -0.7785280 -2.5797040 -1.0550260
 C -3.4970120 0.2474430 0.3987410
 C -1.5726700 2.2627020 0.9834530
 C 6.7392820 -4.4990840 1.8548940
 C -0.6993020 -3.4991620 1.1600610
 C 3.1206200 -1.4236740 0.1950300
 C -4.5126850 1.1417620 0.7496840
 C 3.6087970 5.5178560 3.3077750
 C -2.0047430 1.4585220 -1.7487480
 C -0.8840890 5.4363160 4.8298180
 C -2.1299910 2.2108430 -4.4486440
 C -0.8837660 2.1507510 -3.8269860
 C -0.8557790 1.7730170 -2.4830350
 C -3.7873520 -1.1245130 0.3889620
 C 1.3732870 1.1398780 -2.6118310
 C -1.4987250 -3.9048310 -2.9106810
 C 0.0294440 -2.1384470 2.8899440
 C 2.5919760 1.3955790 0.5565040
 C -1.4403960 -4.8959180 -0.7247000
 C -1.7064270 -4.9961860 -2.1033810
 C -1.6077690 -5.9940980 0.1739750
 C 2.2501830 0.2514170 -1.9842020
 C 1.4566270 1.4742610 -3.9615410
 C -0.7948660 -1.5086200 -3.2302420
 C 3.2643200 -0.3203570 -2.7543620
 C -5.0509820 -1.5867280 0.7093460
 C -0.8537980 -4.6132920 2.0164140
 C -1.3187590 -5.8597370 1.4949780
 C 3.3690580 -0.0112340 -4.1077180
 C -6.0628840 -0.6814210 1.0561880
 C 0.8822470 3.8932490 -4.0326860
 C 4.7957180 -3.5739700 0.8723310

C -1.0070010 4.4144860 2.6940000
 C 2.4656740 3.1439710 2.2376280
 C -5.7867910 0.6912560 1.0770900
 C 3.7687570 1.9898770 0.0660400
 C 1.9497750 1.9972650 1.6348100
 C -1.0915790 3.4739740 0.4731220
 C 5.1390120 -2.2717310 1.2448490
 C 4.2869520 3.1306280 0.6455660
 C -1.7840290 2.1597830 2.3606220
 C -0.8140080 4.5362460 1.3144340
 C 0.3538970 2.4630700 -6.0128800
 C 0.4472210 2.4845050 -4.4909640
 C 2.4738570 0.8735580 -4.7044020
 C 3.6403940 3.7226210 1.7398240
 C -8.3143480 -0.3581960 1.7124970
 C 0.5326350 -0.8051180 3.3315130
 C 4.3035390 -1.2105170 0.9018440
 C 2.7811770 -2.7407420 -0.1602500
 C 3.6069540 -3.8001880 0.1622260
 C -0.5334430 -4.4303500 3.3748510
 C -0.0856810 -3.2045480 3.8045880
 C -1.5082480 3.2201550 3.2178600
 C -3.2367910 1.5492760 -2.4047410
 C -3.2952320 1.9203100 -3.7434290
 C -1.0241600 -2.6971000 -2.3576960
 C -0.9809900 -3.6483580 -0.2453680
 H 6.0495510 -2.0711290 1.7981200
 H 4.5825460 -0.2039290 1.1999430
 H 1.8528670 -2.9282830 -0.6952930
 H 3.3551540 -4.8195190 -0.1134040
 H 7.1664000 -5.4964840 1.9631170
 H 7.4389970 -3.8627360 1.2988900
 H 6.5660820 -4.0681220 2.8490320
 H 1.0150890 1.5938360 2.0011840
 H 1.9324940 3.5878430 3.0666440
 H 5.1908960 3.5962060 0.2658030
 H 4.2767490 1.5548980 -0.7908610
 H 3.5816780 4.8846870 4.2041480
 H 4.2286820 6.3933240 3.5049950
 H 2.5901490 5.8382840 3.0594030
 H -0.2898250 4.6394020 5.2961480
 H -0.5647890 6.4018380 5.2235570
 H -1.9444260 5.2824940 5.0644870
 H -1.6911540 3.1065750 4.2805820
 H -2.1920790 1.2417800 2.7779540
 H -0.4337020 5.4753020 0.9252830
 H -0.9285340 3.5918810 -0.5925090
 H -4.3064180 2.2087530 0.7757600
 H -6.5521890 1.4099000 1.3475460
 H -5.2843000 -2.6467720 0.7070510
 H -3.0058350 -1.8323290 0.1274380
 H -9.1734150 -1.0003850 1.9081650
 H -8.0749880 0.2141010 2.6173430
 H -8.5562780 0.3332270 0.8959030
 H -0.7276500 -1.7960540 -4.2825550
 H -1.6171920 -0.7910970 -3.1260030
 H 0.1291010 -0.9996790 -2.9471160
 H -1.6885350 -3.9564410 -3.9777540

H -2.0649600 -5.9360110 -2.5148810
H -1.9631260 -6.9402500 -0.2243430
H -1.4361510 -6.6964880 2.1777410
H -0.6385010 -5.2606900 4.0680020
H 0.1791270 -3.0411530 4.8440210
H 3.9561260 -1.0189050 -2.2923610
H 4.1558000 -0.4627670 -4.7044810
H 2.5731810 1.0959580 -5.7618510
H 0.0468510 1.4813240 -6.3889590
H -0.3621150 3.2112730 -6.3659130
H 1.3190360 2.7202890 -6.4593480
H 1.8544020 4.1466090 -4.4687620
H 0.1475900 4.6384910 -4.3563080
H 0.9727980 3.9464470 -2.9434050
H -2.1978120 2.4873000 -5.4957260
H -4.2566650 1.9790010 -4.2444170
H -4.1474630 1.3013650 -1.8691550
H 1.5078470 -0.6041480 2.8729380
H -0.1510540 -0.0135050 3.0120360
H 0.6472110 -0.7566620 4.4174240

References

- (1) Van der Veen, L. A., Boele, M. D. K., Bregman, F. R., Kamer, P. C. J., Van Leeuwen, P. W. N. M., Goubitz, K., Fraanje, J., Schenk, H. and Bo, C., *J. Am. Chem. Soc.*, **1998**, *120*, 11616-11626.
- (2) Kranenburg, M., van der Burgt, Y. E. M., Kamer, P. C. J., van Leeuwen, P. W. N. M., Goubitz, K. and Fraanje, J., *Organometallics*, **1995**, *14*, 3081-3089.
- (3) Shaw, L., Somisara, D. M. U. K., How, R. C., Westwood, N. J., Bruijnincx, P. C. A., Weckhuysen, B. M. and Kamer, P. C. J., *Catal. Sci. Technol.*, **2017**, *7*, 619-626.
- (4) Sheldrick, G. M., *Acta Crystallogr., Sect. A: Found. Crystallogr.*, **2008**, *64*, 112-122.
- (5) Sheldrick, G. M., *Acta Crystallogr., Sect. C: Struct. Chem.*, **2015**, *71*, 3-8.
- (6) Macrae, C. F.; Sovago, I.; Cottrell, S. J.; Galek, P. T. A.; McCabe, P.; Pidcock, E.; Platings, M.; Shields, G. P.; Stevens, J. S.; Towler, M. and Wood, P. A. *J. Appl. Crystallogr.* **2020**, *53*, 226-235
- (7) Crosby, G. A. and Demas, J. N., *J. Phys. Chem.*, **1971**, *75*, 991-1024.
- (8) Melhuish, W. H., *J. Phys. Chem.*, **1961**, *65*, 229-235.
- (9) Greenham, N. C., Samuel, I. D. W., Hayes, G. R., Phillips, R. T., Kessener, Y. A. R. R., Moratti, S. C., Holmes, A. B. and Friend, R. H., *Chem. Phys. Lett.*, **1995**, *241*, 89-96.
- (10) Connolly, N. G. and Geiger, W. E., *Chem. Rev.*, **1996**, *96*, 877-910.
- (11) Pavlishchuk, V. V. and Addison, A. W., *Inorg. Chim. Acta*, **2000**, *298*, 97-102.
- (12) Perdew, J. P., Burke, K. and Ernzerhof, M., *Phys. Rev. Lett.*, **1996**, *77*, 3865-3868.
- (13) Perdew, J. P., Burke, K. and Ernzerhof, M., *Phys. Rev. Lett.*, **1997**, *78*, 1396.
- (14) Adamo, C. and Barone, V., *J. Chem. Phys.*, **1999**, *110*, 6158-6170.
- (15) Grimme, S., Antony, J., Ehrlich, S. and Krieg, H., *J. Chem. Phys.*, **2010**, *132*, 154104.
- (16) Grimme, S., Ehrlich, S. and Goerigk, L., *J. Comput. Chem.*, **2011**, *32*, 1456-1465.
- (17) Risthaus, T. and Grimme, S., *J. Chem. Theory Comput.*, **2013**, *9*, 1580-1591.
- (18) Bergner, A., Dolg, M., Küchle, W., Stoll, H. and Preuß, H., *Mol. Phys.*, **1993**, *80*, 1431-1441.
- (19) Miertuš, S., Scrocco, E. and Tomasi, J., *Chem. Phys.*, **1981**, *55*, 117-129.
- (20) Frisch, M. J., Trucks, G. W., Schlegel, H. B., Scuseria, G. E., Robb, M. A., Cheeseman, J. R., Scalmani, G., Barone, V., Mennucci, B., Petersson, G. A., Nakatsuji, H., Caricato, M., Li, X., Hratchian, H. P., Izmaylov, A. F., Bloino, J., Zheng, G., Sonnenberg, J. L., Hada, M., Ehara, M., Toyota, K., Fukuda, R., Hasegawa, J., Ishida, M., Nakajima, T., Honda, Y., Kitao, O., Nakai, H., Vreven, T., Montgomery, J. A., Peralta, J. E., Ogliaro, F., Bearpark, M., Heyd, J. J., Brothers, E., Kudin, K. N., Staroverov, V. N., Kobayashi, R., Normand, J., Raghavachari, K., Rendell, A., Burant, J. C., Iyengar, S. S., Tomasi, J., Cossi, M., Rega, N., Millam, J. M., Klene, M., Knox, J. E., Cross, J. B., Bakken, V., Adamo, C., Jaramillo, J., Gomperts, R., Stratmann, R. E., Yazyev, O., Austin, A. J., Cammi, R., Pomelli, C., Ochterski, J. W., Martin, R. L., Morokuma, K., Zakrzewski, V. G., Voth, G. A., Salvador, P., Dannenberg, J. J., Dapprich, S., Daniels, A. D., Foresman, J. B., Ortiz, J. V., Cioslowski, J. and Fox, D. J., *Gaussian09 (Revision D.01)*, **2013**, Gaussian Inc.
- (21) Runge, E. and Gross, E. K. U., *Phys. Rev. Lett.*, **1984**, *52*, 997-1000.
- (22) Becke, A. D., *J. Chem. Phys.*, **1993**, *98*, 1372-1377.
- (23) Lee, C., Yang, W. and Parr, R. G., *Phys. Rev. B* **1988**, *37*, 785-789.
- (24) Yanai, T., Tew, D. P. and Handy, N. C., *Chem. Phys. Lett.*, **2004**, *393*, 51-57.
- (25) Stevens, W. J., Krauss, M., Basch, H. and Jasien, P. G., *Can. J. Chem.*, **1992**, *70*, 612-630.
- (26) Smith, C. S., Branham, C. W., Marquardt, B. J. and Mann, K. R., *J. Am. Chem. Soc.*, **2010**, *132*, 14079-14085.
- (27) McNitt, K. A., Parimal, K., Share, A. I., Fahrenbach, A. C., Witlicki, E. H., Pink, M., Bediako, D. K., Plaisier, C. L., Le, N., Heeringa, L. P., Griend, D. A. V. and Flood, A. H., *Journal of the American Chemical Society*, **2009**, *131*, 1305-1313.
- (28) Pal, A. K., Li, C., Hanan, G. S. and Zysman-Colman, E., *Angew. Chem., Int. Ed.*, **2018**, *57*, 8027-8031.
- (29) Quaranta, M., Murkovic, M. and Klimant, I., *Analyst*, **2013**, *138*, 6243-6245.
- (30) Sheldrick, G. M. *Acta Crystallogr., Sect. A*, **2015**, *71*, 3-8.

- (31) Spek, A. L. *Acta Crystallogr. Sect C*. 2015, **71**, 9-18.
- (32) Spek, A. L. *Acta Crystallogr. Sect D*. 2009, **65**, 148-155.